



HAL
open science

New paleomagnetic and geochronologic results from Ethiopian Afar: Block rotations linked to rift overlap and propagation and determination of a 2 Ma reference pole for stable Africa

T Kidane, Vincent Courtillot, Isabelle Manighetti, L Audin, P Lahitte, X Quidelleur, Y Gillot, Y Gallet, J Carlut, T Haile

► To cite this version:

T Kidane, Vincent Courtillot, Isabelle Manighetti, L Audin, P Lahitte, et al.. New paleomagnetic and geochronologic results from Ethiopian Afar: Block rotations linked to rift overlap and propagation and determination of a 2 Ma reference pole for stable Africa. *Journal of Geophysical Research : Solid Earth*, 2003, 22, pp.491 - 491. 10.1029/2001JB000645 . insu-01570942

HAL Id: insu-01570942

<https://insu.hal.science/insu-01570942>

Submitted on 1 Aug 2017

HAL is a multi-disciplinary open access archive for the deposit and dissemination of scientific research documents, whether they are published or not. The documents may come from teaching and research institutions in France or abroad, or from public or private research centers.

L'archive ouverte pluridisciplinaire **HAL**, est destinée au dépôt et à la diffusion de documents scientifiques de niveau recherche, publiés ou non, émanant des établissements d'enseignement et de recherche français ou étrangers, des laboratoires publics ou privés.

New paleomagnetic and geochronologic results from Ethiopian Afar: Block rotations linked to rift overlap and propagation and determination of a ~ 2 Ma reference pole for stable Africa

Tesfaye Kidane,^{1,2} Vincent Courtillot,¹ Isabelle Manighetti,¹ Laurence Audin,^{1,3} Pierre Lahitte,⁴ Xavier Quidelleur,^{1,4} Pierre-Yves Gillot,⁴ Yves Gallet,¹ Julie Carlut,⁵ and Tigistu Haile²

Received 25 May 2001; revised 16 July 2002; accepted 22 August 2002; published 18 February 2003.

[1] Joint French–Ethiopian field trips in 1995–1996 yield new geochronologic and paleomagnetic data, which significantly expand our knowledge of the recent magmatic and tectonic history of the Afar depression. Twenty-four new K–Ar ages range from 0.6 to 3.3 Ma. There is quite good agreement between magnetic polarities and Geomagnetic Polarity Timescale (GPTS). Eight age determinations with uncertainty less than 50 kyr can be used in future reassessments of the GPTS (upper and lower Olduvai/Matuyama reversals and Reunion and Mammoth subchrons). Paleomagnetic analysis of 865 cores from 133 sites confirms that low-Ti magnetites are the main carrier of the Characteristic Remanent Magnetization (ChRM). A positive tilt test (based on two subgroups with 63 and 23 sites, respectively) confirms that this ChRM is likely the primary magnetization. The main paleomagnetic results can be summarized as follows. A ~ 2 Ma reference pole for stable Africa is determined based on 26 sites located on either side of the northern termination of the East African rift. It is located at $\lambda = 87.2^\circ\text{N}$, $\phi = 217.1^\circ\text{E}$ ($A_{95} = 4^\circ$). A $4.6 \pm 1.8^\circ$ (2σ) inclination shallowing is identified within a population of 231 stratoid lava flows, consistent with a global axial quadrupole of $6 \pm 2\%$ of the axial dipole. Combined with earlier data of *Acton et al.* [2000], our new data allow mean paleomagnetic field directions to be determined for five individual, fault-bounded blocks previously identified by tectonic analysis within central Afar. These all have suffered negligible rotations about vertical axes since emplacement of the lava. This contrasts with the significant rotations previously uncovered to the east in Djiboutian Afar for three major individual blocks. Taken altogether, the declination differences with respect to reference directions are $2 \pm 4^\circ$ for central Afar and $13 \pm 4^\circ$ for eastern Afar, consistent with the model of *Manighetti et al.* [2001a]. It appears that in the last ~ 3 Ma the Afar depression was extensively flooded by trap-like basalts, which were deformed by a single but complex physical (tectonic) process, combining diffuse extension, rift localization, propagation, jumps and overlap, and bookshelf faulting. **INDEX TERMS:** 1525 Geomagnetism and Paleomagnetism: Paleomagnetism applied to tectonics (regional, global); 1035 Geochemistry: Geochronology; 8109 Tectonophysics: Continental tectonics—extensional (0905); 3040 Marine Geology and Geophysics: Plate tectonics (8150, 8155, 8157, 8158); 9604 Information Related to Geologic Time: Cenozoic; **KEYWORDS:** Afar tectonics, block rotation, rift propagation and overlap, reference pole, polarity timescale, inclination anomaly

Citation: Kidane, T., V. Courtillot, I. Manighetti, L. Audin, P. Lahitte, X. Quidelleur, P.-Y. Gillot, Y. Gallet, J. Carlut, and T. Haile, New paleomagnetic and geochronologic results from Ethiopian Afar: Block rotations linked to rift overlap and propagation and determination of a ~ 2 Ma reference pole for stable Africa, *J. Geophys. Res.*, 108(B2), 2102, doi:10.1029/2001JB000645, 2003.

¹Laboratoires de Paléomagnétisme et de Tectonique, Institut de Physique du Globe de Paris, Paris, France.

²Department of Geology and Geophysics, University of Addis-Ababa, Addis-Ababa, Ethiopia.

³Institut de Recherche pour le Développement, Université Paul Sabatier, Géologie, Toulouse, France.

⁴Laboratoire de Géochronologie Multi-Techniques, Université Paris Sud–Institut de Physique du Globe de Paris, Sciences de la Terre, Université Paris XI-Paris Sud, Orsay, France.

⁵Laboratoire de Géologie, Ecole Normale Supérieure, Paris, France.

1. Introduction

[2] The Afar depression is one of the best field laboratories where the early stages of continental breakup and the onset of seafloor spreading can be studied in the field. After the initial discovery that the Aden rift propagated onland into Afar [e.g., *Courtillot*, 1980, 1982; *Courtillot et al.*, 1980, 1987], and the finding that rather large block rotations due to rift propagation could be directly measured using paleomagnetic techniques [*Courtillot et al.*, 1984], continued fieldwork within the Republic of Djibouti between 1989 and 1993 led to the

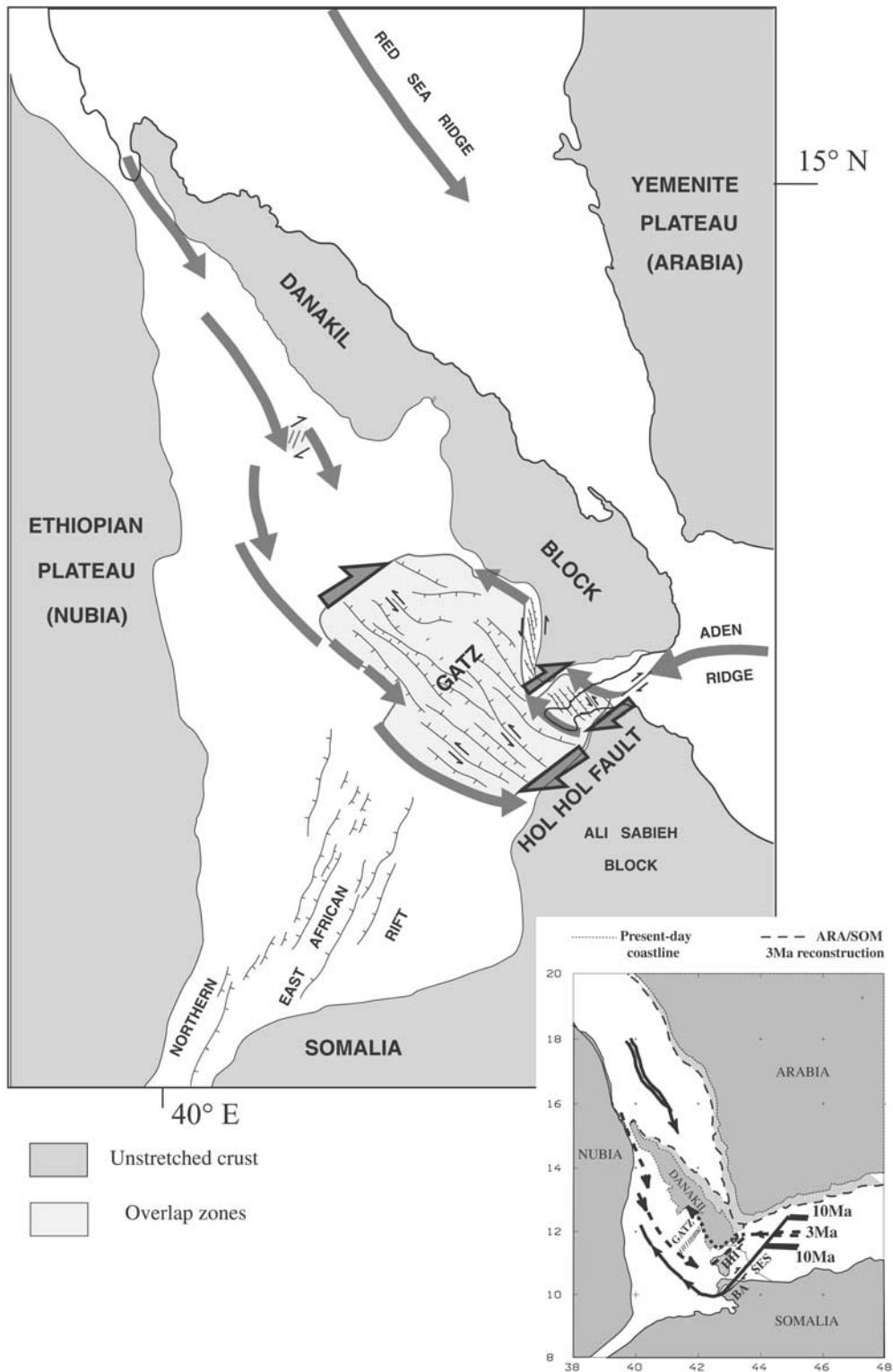


Figure 1. Tectonic framework of rift propagation around the Afar depression [Manighetti *et al.*, 2001a]. Large full arrows are for rifts and half arrowheads for coeval shear zones. Inset: Relative locations (with respect to the African, i.e., Nubia/Somalia, plate) of the Danakil block and Arabian plate at Present (dark shade) and 3 Ma ago (light shade) [Audin, 1999]. SES: Shukra-el-Sheik transform fault; BA: Bia Anot fault; HH: Hol Hol fault; GATZ: Gambarri-Alol tear zone (see text).

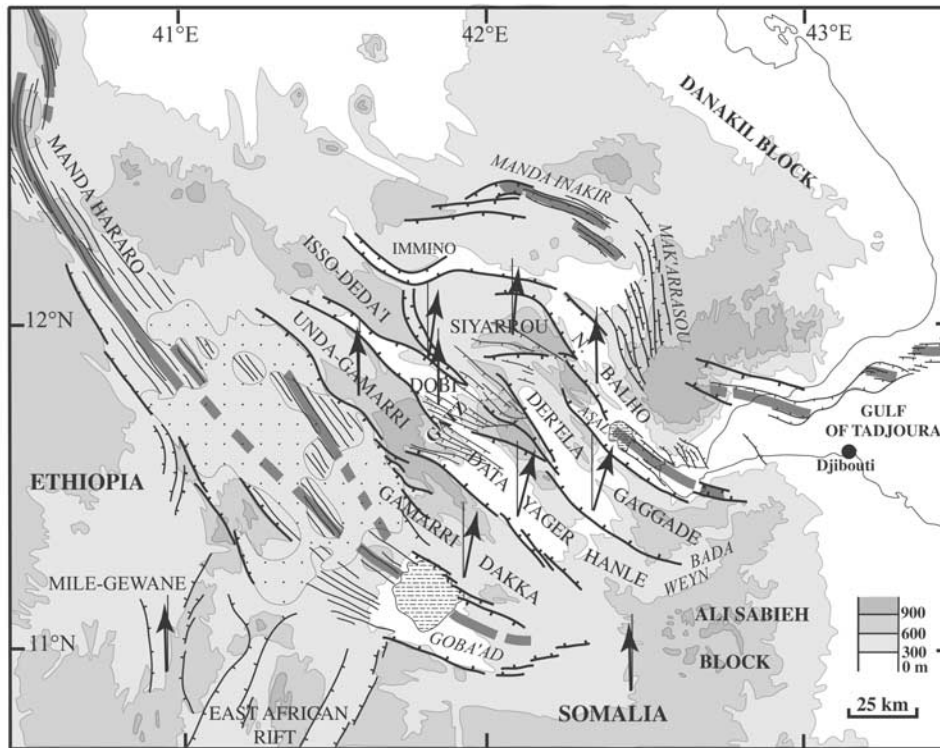


Figure 2. Details of rift and block structure in Afar [Manighetti *et al.*, 2001a], with rift segments (broad gray lines), main faults, and an indication of individual block rotations measured from paleomagnetism in the present and earlier studies.

publication of a series of papers on the propagation of rifting in the gulfs of Aden and Tadjoura [Manighetti *et al.*, 1997] and into Afar [Manighetti *et al.*, 1998], ending with a model for the history of strain transfer between overlapping propagating rifts [Manighetti *et al.*, 2001a].

[3] Eruption of the Ethiopian traps about 30 Ma ago [e.g., Baker *et al.*, 1972; Hofmann *et al.*, 1997; Rochette *et al.*, 1998] facilitated breakup of Arabia and Africa [Courtilot *et al.*, 1999] and, after an initial phase of incipient breakup along the East African rift and the Red Sea, the Gulf of Aden rift propagated from the Indian ocean toward the area weakened by the hot spot; it arrived on the Shukra-el-Sheik discontinuity about 20 Ma ago, where it stalled for some 13 Ma (Figure 1, inset) [Manighetti *et al.*, 1997; Audin, 1999]. In the mean time (~ 30 –20 Ma), the Red Sea rift had propagated toward the hot spot area. There, the lithosphere was so softened that both rifts were unable to break it in a clean-cut fashion; the Afar depression started to stretch through both localized (disconnected rift segments) and diffuse faulting, associated with magmatism. Two “microplates,” the Danakil and Ali Sabieh blocks, were isolated and the depression started opening (Figure 1). Since about 1 Ma, the Aden rift has localized along the western edge of the Danakil block, where it has been propagating northward in a series of discontinuous jumps. In the process, a large size, growing overlap was formed (Figure 1) [e.g., Manighetti, 1993; Audin, 1999; Manighetti *et al.*, 1998, 2001a].

[4] Transient deformation in the growing overlap zone occurred through distributed extensional faulting and rotation of a small number of “miniblocks,” following a bookshelf faulting mechanism (Figure 1) [Tapponnier *et*

al., 1990; Manighetti *et al.*, 2001a, 2001b]. The strain history can be accounted for in terms of rotations about vertical axes of small rigid blocks, but since it is transient these blocks can be defined only for a certain time span, on the order of a few hundred thousand years [Manighetti *et al.*, 2001a]. Two recent phases of deformation, propagation, and overlap have been identified: during the first phase, fault-bounded blocks rotated and stretched. During this time, westward and northward propagation continued, establishing the Mak’arrasou transform zone and triggering rifting in the Manda-Inakir rift (Figure 2). As a result, the bookshelf mechanism propagated west.

[5] Rift formation and propagation were accompanied by volcanism. The oldest formation, the Adolei basalts, is found in the Ali-Sabieh region, at the current southern margin of the depression and is dated at ~ 27 Ma [Barberi *et al.*, 1975; Black *et al.*, 1975]. This volcanic activity may have lasted some ≈ 8 Myr [Deniel *et al.*, 1994], and was followed from ~ 16 to ~ 9 Ma by emplacement of the Mabla rhyolites [Varet *et al.*, 1975; Chessex *et al.*, 1975]. A new basaltic phase erupted ~ 8 to ~ 4 Ma ago, known as the Dahla basalts [Varet and Gasse, 1978]. All of the above formations outcrop only over limited surfaces near the edges of the depression.

[6] The most important formation is the 1–1.5 km thick basaltic stratoid series which floors more than 2/3 of the depression [Varet *et al.*, 1975]. Conventional K-Ar dating assigned it ages from 0.4 to 4.4 Ma [Barberi *et al.*, 1972, 1975; Civetta *et al.*, 1975; Chessex *et al.*, 1975; Black *et al.*, 1975]. Further K-Ar and ^{40}Ar – ^{39}Ar ages, restricted to the southeastern part of the depression in the Republic of Djibouti, were in a window from 1.3 to 2.2 Ma [Courtilot

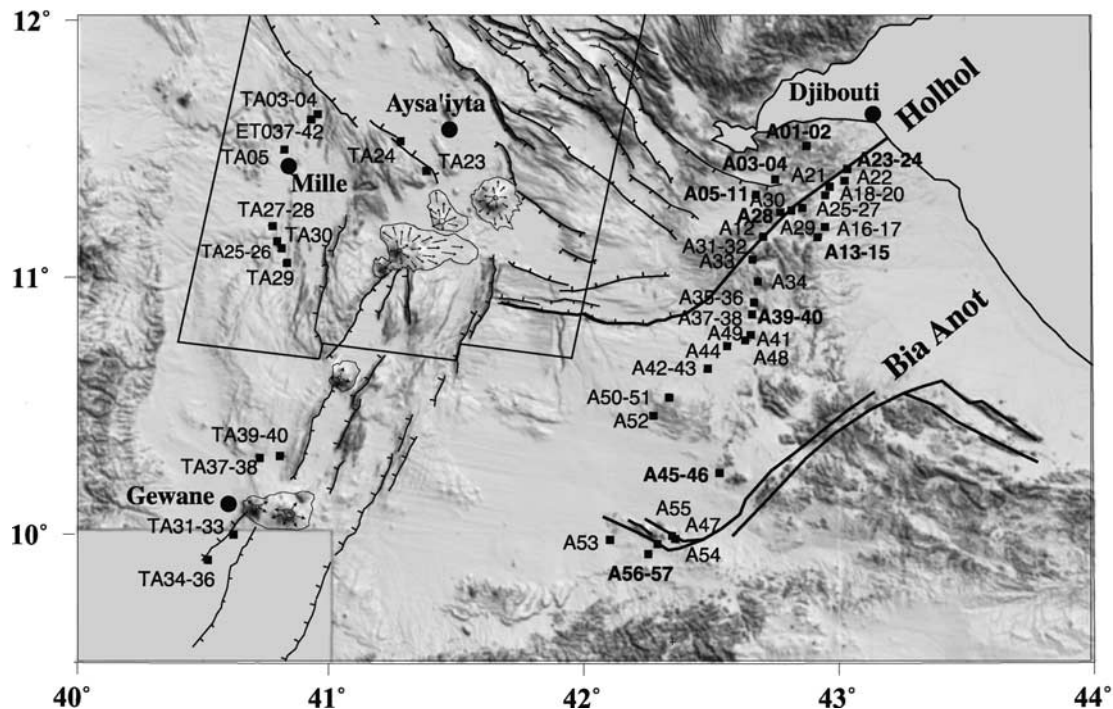


Figure 3a. Map of the studied area, with sites (shown as squares) sampled for paleomagnetism and age determination. Main faults are indicated. Towns are shown as full circles. All sites cannot be shown in the area with densest sampling in central Afar, which is shown in more detail in Figures 3b and 3c.

et al., 1984]. These authors suggested that peak phases of basaltic volcanism were episodic in nature, with alternating ~ 1 Ma long phases of volcanism and tectonic deformation.

[7] The model of *Manighetti et al.* [2001a] was largely based on data restricted to the Republic of Djibouti, and on geophysical data from the oceanic part of the gulf of Aden. Yet, it makes predictions for the remaining largest part of the Afar depression, which occurs mostly within Ethiopia. Testing of this model is possible through combination of field and remote tectonic analyses, paleomagnetic and geochronological sampling. With such testing in mind, a collaboration program was established between INSU-CNRS and the department of geology and geophysics of the University of Addis-Ababa and fieldwork started in 1995. Sampling was focused on the stratoid series. Data obtained on older formations are included in the study of L. Audin *et al.* (Paleomagnetic constraints and timing of deformation associated with the onland propagation of the Aden ridge into SE Afar during the last 8 Myr, submitted manuscript, 2002, hereinafter referred to as Audin *et al.*, submitted manuscript, 2002), and additional new data and a critical review of all geochronological results are given by *Lahitte et al.* [2001].

[8] Our aim was to sample as densely as possible the blocks identified in the remote sensing tectonic analyses, in order to constrain their ages and rotations. Another goal was to sample the less deformed, “stable” part of African crust, since all rotations measured previously in the Republic of Djibouti could only be referred to a “synthetic” African reference but not to actual African data. The fieldwork on which the present paper focuses was undertaken in 1995 and 1996, and the analytical work is described in detail by

Kidane [1999]. Independent work had been undertaken in the field by Gary Acton and colleagues in 1992 and was published by *Acton et al.* [2000]. The two data sets are complementary and will be combined in this paper. Additional analyses are given by *Audin* [1999] [see also Audin *et al.*, submitted manuscript, 2002] with an emphasis on tectonic data, and by *Lahitte* [2000] [see also *Lahitte et al.*, 2001] with an emphasis on geochronological data.

[9] We first recall some geological information, then describe our geochronological results, next the paleomagnetic results, and discuss all these jointly in the frame of the *Manighetti et al.* [2001a] and *Acton et al.* [1991, 2000] models. At the same time we provide a new ~ 2 Ma reference paleomagnetic pole for “stable” Africa.

2. Geological Constraints and Tectonic Microblocks

[10] Figure 2 displays a simplified topographic and tectonic map of the central part of the Afar depression. Based on previous inspection of satellite and air photographs and fieldwork, a number of active rift segments and major faults were identified. Analyses of fault size, geometry and displacement, scarp morphology, offset markers, and evidence of recent seismic activity reveal a hierarchy of tectonic features [*Manighetti*, 1993] and define a limited number of microblocks.

[11] In the eastern part of the area, largely within the Republic of Djibouti, one encounters a series of roughly NW-SE-striking normal faults, most of them with a significant component of left-lateral slip. These faults bound a series (5–9 according to *Manighetti et al.* [2001a]) of much

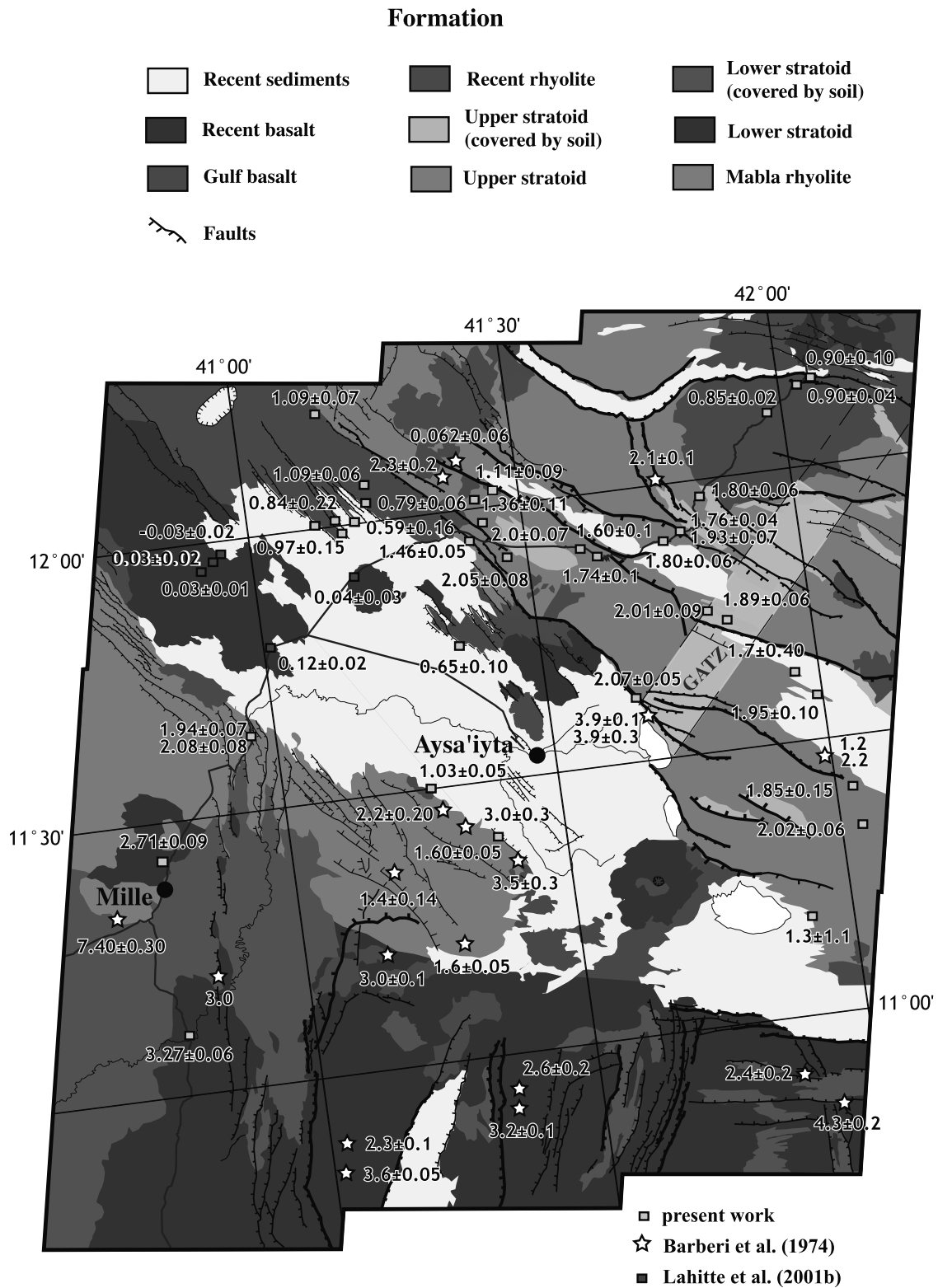


Figure 3b. Geological map of central Afar with main formations and faults and location of sites where an age determination has been obtained (yellow squares: K-Ar determinations (this study and earlier ones by our group); red squares: thermoluminescence data [Lahitte et al., 2003]; stars: K-Ar determinations [Barberi et al., 1975]; GATZ: Gamarrri Alol tear zone. See color version of this figure at back of this issue.

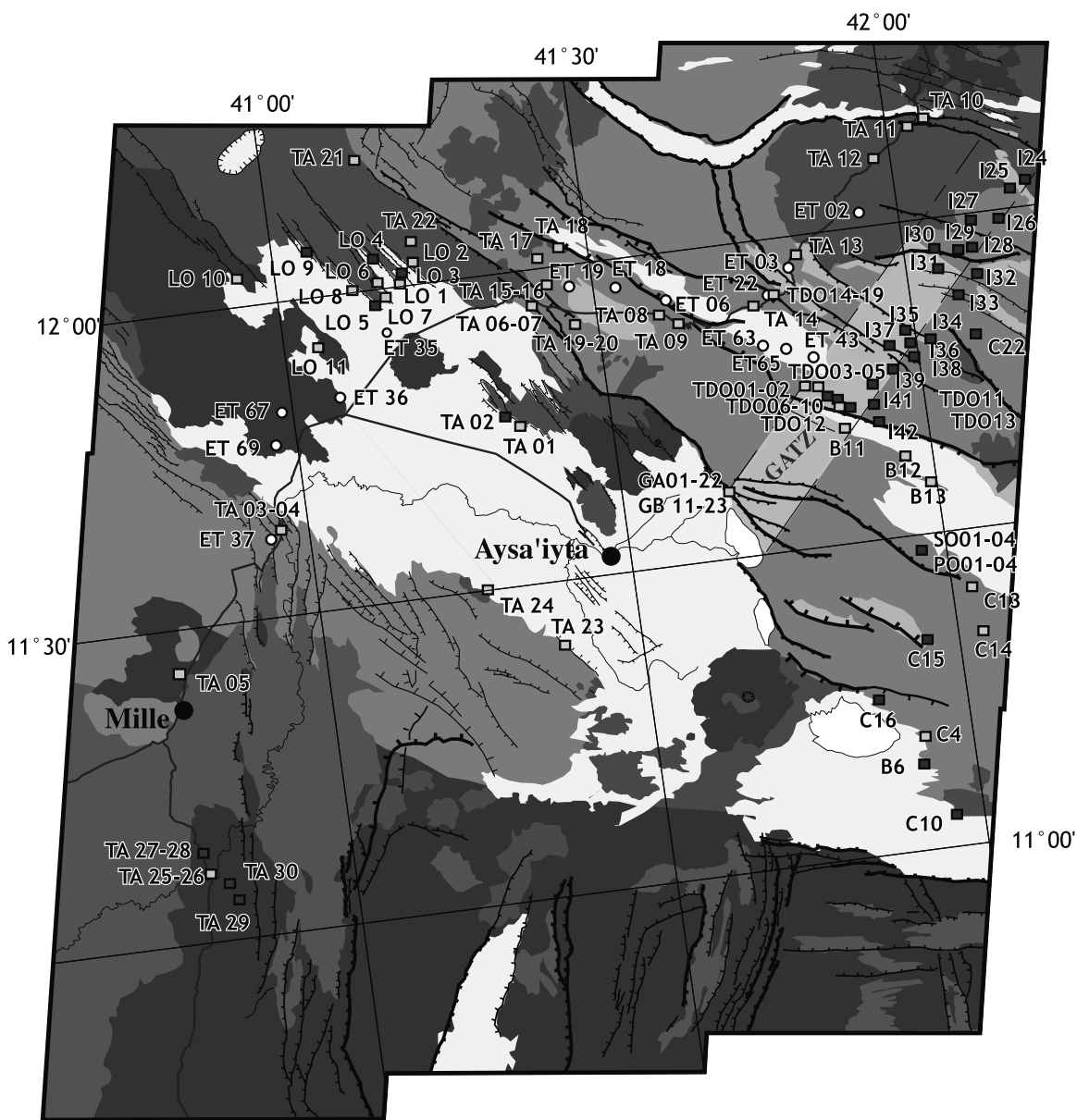


Figure 3c. Same as Figure 3b, with location of paleomagnetic sites: open circles are from the study of *Acton et al.* [2000]; squares are from our group [*Courtilot et al.*, 1984; *Manighetti*, 1993; *Manighetti et al.*, 2001a; this paper]: yellow squares are sites with a joint age determination and red squares are without one. See color version of this figure at back of this issue.

less deformed blocks, with from south to north three major, first-order blocks: Gambari-Dakka, Data-Yager-Hanle, and Der'Ela-Gaggade. The identification of the northwestern termination of these blocks has been the subject of work by *Manighetti* [1993]. The blocks terminate in a tapered fashion through a series of en échelon fault segments with evidence of strike slip motion. All eventually terminate along the Gambari-Alol tear zone (GATZ) [see also *Manighetti et al.*, 2001a]. To the SE, the mean strike of the faults rotates to a more EW azimuth, and the faults are apparently rooted in the hardy deformed Ali Sabieh block.

[12] North of the Asal-Ghoubbet active rift system, one encounters the Mak'arrasou transfer zone, along which strain is transferred further north to the next, younger,

propagating Manda-Inakir rift. A small block (north Balho) can be defined between the NW extension of the Ghoubbet-Asal southern bordering fault, the Gambari-Alol tear zone, the Mak'arrasou transfer zone and the Manda-Inakir rift.

[13] Related blocks can be described to the west of GATZ. Again going from south to north, one first encounters the "stable" edge of the Ethiopian (African) plate, the active Manda-Hararo rift which forms the southern extension of the Red Sea propagating rift system, the Unda-Gambari block, the small Dobi sliver, the larger Isso-Deda'i/Siyarrou block bounded to the north by the conspicuous, S-shaped Immino graben, followed to the north by the north Immino block until the western termination of the Manda-Inakir rift.

Table 1. Results of K-Ar Dating of 24 Basaltic Lava Flows From the Afar Depression^a

Sample	K%	Percentage of ⁴⁰ Ar*	⁴⁰ Ar*, at./g ($\times 10^{11}$)	Age, Ma	Uncertainty (1 σ Level)	Magnetic Polarity
70J	0.339	0.429	2.6732	0.75	0.26	L01
	0.339	0.722	1.7405	0.49	0.10	Reversed
72B	0.428	0.930	2.6078	0.583	0.094	TA01
	0.428	1.061	3.2041	0.717	0.102	Transitional
70K	0.307	1.840	2.9028	0.91	0.07	L02
	0.307	2.213	2.2539	0.70	0.05	Reversed
70L	0.377	0.410	4.3829	1.11	0.41	L06C1
	0.377	0.859	2.8294	0.72	0.13	Reversed
72L	0.796	6.709	7.1690	0.862	0.023	TA12
	0.796	7.090	6.9692	0.838	0.021	Reversed
72K	0.818	3.800	8.1795	0.96	0.04	TA11
	0.818	3.64	7.7704	0.91	0.04	Reversed
72J	0.543	1.679	5.0987	0.899	0.081	TA10
	0.543	1.440	5.6175	0.990	0.104	Normal
70N	0.307	0.176	1.9058	0.60	0.51	L083
	0.307	1.422	3.2667	1.02	0.11	Normal
72W	0.303	3.500	3.2429	1.02	0.05	TA24
	0.303	2.640	3.3140	1.05	0.06	Reversed
72U	0.922	2.500	9.9720	1.04	0.06	TA22
	0.922	3.000	10.8900	1.13	0.06	Reversed
72T	0.865	2.350	9.9646	1.10	0.07	TA21
	0.865	2.290	9.7682	1.08	0.07	Reversed
72Q	0.882	1.770	10.2070	1.11	0.10	TA18
	0.882	1.740	10.2520	1.11	0.10	
72P	0.679	1.600	8.4826	1.20	0.11	Reversed
	0.679	2.070	10.9920	1.55	0.11	
72C	0.743	4.050	11.6700	1.50	0.06	TA06
	0.743	4.680	11.1240	1.43	0.05	Reversed
72V	1.053	4.700	16.8450	1.53	0.05	TA23
	1.053	5.450	17.5860	1.60	0.05	Reversed
72H	0.873	6.490	14.6700	1.61	0.04	TA08
	0.873	6.940	14.5400	1.59	0.04	Reversed
72I	1.014	2.940	18.9940	1.79	0.09	TA09
	1.014	2.710	17.9130	1.69	0.10	Reversed
72M	1.494	4.430	26.9980	1.73	0.06	TA13
	1.494	5.456	28.1030	1.80	0.06	Reversed
72N	0.790	4.380	14.6900	1.78	0.07	TA 14
	0.790	4.950	15.0360	1.82	0.06	Normal
72D1	0.802	4.994	16.6040	1.98	0.07	TA03
	0.802	4.409	15.9570	1.90	0.07	Reversed
72O	0.973	4.470	20.4260	2.01	0.07	TA15
	0.973	4.850	20.2080	1.99	0.07	Reversed

Table 1. (continued)

Sample	K%	Percentage of ⁴⁰ Ar*	⁴⁰ Ar*, at./g (×10 ¹¹)	Age, Ma	Uncertainty (1σ Level)	Magnetic Polarity
72R	1.029	4.200	21.4550	2.00	0.08	TA20
	1.029	4.160	22.5340	2.10	0.08	Reversed
72D2	0.750	4.048	16.1160	2.06	0.08	TA04
	0.750	4.684	16.3970	2.09	0.07	Reversed
				2.08	0.08	
				2.75	0.10	TA05
72E	0.200	4.560	5.7436	2.68	0.08	Normal
	0.200	5.310	5.6069	2.71	0.09	

^aSample, identification; K%, total percentage of potassium in sample; percentage of ⁴⁰Ar*, percentage of radiogenic argon 40 in sample; ⁴⁰Ar*, at./g, number of atoms of radiogenic argon 40 per gram of sample (in 10¹¹ at/g); Age, Ma, ages determined from two replicate argon measurements for each sample (the means of these replicate determinations are given in bold); uncertainty is at the 1σ level; corresponding magnetic polarity at same site (paleomagnetic site code is given) is also indicated.

[14] Earlier sampling in the Republic of Djibouti provided extensive paleomagnetic and geochronological data sets on the Gamarri-Dakka, Data-Yager-Hanle, and Der'Ela-Gaggade blocks, except for their northwestern terminations [Galibert *et al.*, 1980; Courtillot *et al.*, 1984; Manighetti, 1993; Manighetti *et al.*, 2001a]. Detailed work on a section of the Gamarri fault and escarpment on the Ethiopian side (GA and GB sites in Figure 3c) has been

reported elsewhere [Kidane *et al.*, 1999]. Work by Acton *et al.* [2000] has concentrated along (and up to 3 km away from) the only Highway and resulted in 48 paleomagnetic stratoid sites (labeled ET in Figure 3c; 350 analyzed cores, without geochronological data; sites discussed but rejected by the authors are not mentioned here). These sites are located mainly on the Manda-Hararo rift, and the Unda Gamarri, Dobi, Isso, Siyarrou, and north Immino blocks.

Table 2. Location, Previous and Proposed Geological Formation Assignment, and Ages of Samples Listed in Table 1 and Published by Kidane *et al.* [1999] and Lahitte [2000] and Collected Along or Close to the Main Addis Ababa-Asab Road

Sample Name	Locality	Lat, Lon, deg	Formation (Previous)	Age ± 1σ Uncertainty, Ma	Formation (This Study)	Block
70J ^a	NW of Serdo	12.017, 41.205	Stratoid series	0.59 ± 0.16	Gulf basalt	Serdo-Semera
72B ^a	North of Aysaita	11.782, 41.343	Upper stratoid	0.65 ± 0.10	Gulf basalt	Manda-Hararro
75CF ^b	Near Gewane	10.000, 40.600	Stratoid series	0.73 ± 0.06	Gulf basalt	Ethiopian Plate
70K ^a	NW of Serdo	12.033, 41.225	Stratoid series	0.79 ± 0.06	Gulf basalt	Serdo-Semera
70L ^a	NW of Serdo	12.019, 41.178	Stratoid series	0.84 ± 0.22	Gulf basalt	Serdo-Semera
72L ^a	NE of Elidar	12.096, 41.982	Upper stratoid	0.85 ± 0.02	Gulf basalt	Siyarrou
72K ^a	Immino graben	12.153, 42.056	Upper stratoid	0.94 ± 0.04	Gulf basalt	Siyarrou
72J ^a	Immino graben	12.152, 42.056	Upper stratoid	0.94 ± 0.09	Gulf basalt	Siyarrou
70N ^a	NW of Serdo	12.022, 41.133	Stratoid series	0.97 ± 0.15	Gulf basalt	Serdo-Semera
72W ^a	South of Datbahri	11.525, 41.261	Upper stratoid	1.03 ± 0.05	Gulf basalt	Ethiopian Plate
72U ^a	North of Serdo	12.087, 41.250	Stratoid series	1.09 ± 0.06	Gulf basalt	Unda-Gamarri
72T ^a	NW of Serdo	12.223, 41.179	Stratoid series	1.09 ± 0.07	Gulf basalt	Serdo-Semera
72Q ^a	North of Dichooto	12.041, 41.449	Stratoid series	1.11 ± 0.09	Gulf basalt	Unda-Gamarri
72P ^a	NW Dichooto	12.042, 41.436	Stratoid series	1.36 ± 0.11	Upper stratoid	Unda-Gamarri
72C ^a	Around Serdo	11.956, 41.533	Stratoid series	1.46 ± 0.05	Upper stratoid	Unda-Gamarri
72V ^a	South of Datbahri	11.413, 41.356	Stratoid series	1.57 ± 0.05	Upper stratoid	Ethiopian Plate
2H ^a	East of Dichooto	11.917, 41.587	Stratoid series	1.60 ± 0.04	Upper stratoid	Unda-Gamarri
72I ^a	East of Dichooto	11.893, 41.650	Stratoid series	1.74 ± 0.10	Upper stratoid	Unda-Gamarri
75AJ1 ^b	South of Isso	11.917, 41.783	Stratoid series	1.76 ± 0.04	Upper stratoid	Isso-Deda'ai
72M ^a	Around Elidar	11.969, 41.838	Stratoid series	1.77 ± 0.06	Upper stratoid	Siyarrou
72N ^a	Dobi Escarp.	11.895, 41.759	Stratoid series	1.80 ± 0.06	Upper stratoid	Dobi
75D ^a	Dobi graben	11.760, 41.823	Stratoid series	1.89 ± 0.06	Upper stratoid	Dobi
75AJ2 ^b	South of Isso	11.917, 41.783	Stratoid series	1.93 ± 0.07	Upper stratoid	Isso-Deda'ai
72D1 ^a	SW of Serdo	11.624, 40.939	Stratoid series	1.94 ± 0.07	Upper stratoid	Ethiopian Plate
72O ^a	NW Dichooto	11.981, 41.434	Stratoid series	2.00 ± 0.07	Upper stratoid	Unda-Gamarri
75B1 ^b	Dobi graben	11.803, 41.759	Stratoid series	2.01 ± 0.09	Upper stratoid	Dobi
GB23 ^c	Gamarri Sect.	11.600, 41.700	Stratoid series	2.02 ± 0.04	Upper stratoid	Gamarri-Dakka
GA22 ^c	Gamarri Sect.	11.600, 41.700	Stratoid series	2.03 ± 0.08	Upper stratoid	Gamarri-Dakka
72R ^a	West of Dichooto	11.925, 41.469	Stratoid series	2.05 ± 0.08	Upper stratoid	Unda-Gamarri
72D2 ^a	SW of Serdo	11.624, 40.939	Stratoid series	2.08 ± 0.08	Upper stratoid	Ethiopian Plate
GB30 ^c	Gamarri Sect.	11.600, 41.700	Stratoid series	2.08 ± 0.06	Upper stratoid	Gamarri-Dakka
GA10 ^c	Gamarri Sect.	11.600, 41.700	Stratoid series	2.09 ± 0.06	Upper stratoid	Gamarri-Dakka
GA02 ^c	Gamarri Sect.	11.600, 41.700	Stratoid series	2.14 ± 0.06	Upper stratoid	Gamarri-Dakka
72E ^a	North of Mille	11.496, 40.799	Dahla basalt	2.71 ± 0.09	Lower stratoid	Ethiopian Plate
75CC ^b	North of Gewane	10.300, 40.800	Stratoid series	3.22 ± 0.19	Lower stratoid	Ethiopian Plate
75CB1 ^b	Near Adaytu	11.125, 40.775	Stratoid series	3.27 ± 0.06	Lower stratoid	Ethiopian Plate

^aThis paper.

^bLahitte [2000].

^cKidane *et al.* [1999].

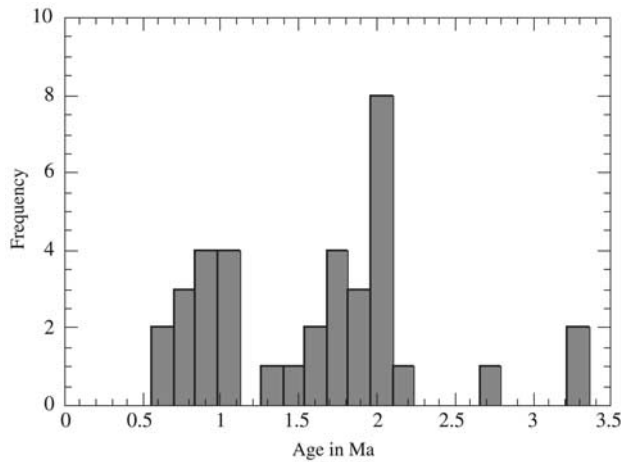


Figure 4. Histogram of 36 age determinations given in this paper (see Table 2).

We collected 133 sites (865 cores collected, 728 analyzed for paleomagnetism, 24 samples for geochronology; Figures 3a–3c), providing paleomagnetic and geochronological data on a wider surface than previously available, sampling all blocks referred to previously west of the Gamarri-Alol tear zone, and the (possibly) stable parts of the African plate, on both sides of the northernmost termination of the East African rift (which we will call Mile-Gewane and Ali-Sabieh, respectively; see Figure 2) [see *Audin*, 1999].

3. Geochronology

[15] We collected a series of 24 new samples on outcrops previously assigned to the stratoid series (Figure 3b). This was complemented by more detailed analyses of the so-called Gamarri cliff (Figure 3c), where five samples from a continuous magnetostratigraphic section provided consistent ages (2.07 ± 0.05 Ma) [*Kidane et al.*, 1999]. Additional samples covering a broader temporal range have been analyzed by *Lahitte et al.* [2001, 2003].

[16] All this new dating was performed using the Cassinot-Gillot K-Ar technique [*Cassinot and Gillot*, 1982; *Gillot and Cornette*, 1986]. Great care was taken in sampling only fresh rocks in the field. Although sampling was performed essentially along fault scarps, which may have been affected by fluid circulation, selected samples were from massive lavas with microlithic groundmass. The groundmass was systematically selected for sample preparation by means of heavy liquids separation, after careful examination in thin section. Samples with doleritic textures were rejected. Further details are given by *Gillot and Cornette* [1986]. The GL-O standard [*Odin*, 1982] and the conventional international decay constants [*Steiger and Jäger*, 1977] were used throughout.

[17] The results of our 24 measurements are given in Table 1. All have been duplicated on separate aliquots. In the following discussion, 12 results obtained earlier in the Gamarri section [*Kidane et al.*, 1999] and by *Lahitte* [2000] are also included (Table 2). Ages range from ~ 0.6 to ~ 3.3 Ma. The data histogram (Figure 4) suggests three unequal

age groups: 13 samples within 0.6–1.1 Ma, 20 between 1.3 and 2.2 Ma, and 3 older than 2.5 Ma.

[18] Given field and aerial photographs, we can separate the “stratoid” series into three distinct age subgroups characterized by different overall texture, freshness, and degree of incision. We call these subgroups the lower and upper stratoid formations and the “Gulf” basalts (following existing usage). The lower stratoid formation is defined by only 3 dated samples between 2.6 and 3.3 Ma, outcropping near the northern termination of the East African rift system (Figures 3a and 3b). It has flat topography and tabular surfaces, and outcrops along river cuts and gullies. It is also exposed along the shores of the Awash river. The characteristic morphology and topography allows the mapping shown in Figures 3b and 3c.

[19] The upper stratoid formation outcrops north of Mile. Good exposures occur mainly along fault scarps. Lava flows are tabular with large-scale horizontal continuity. Around 50% of the region we studied is covered by this formation. It is the most widespread and thickest formation found in the depression, with a thickness reaching at least 1500m. Lava flows are continuous and sometimes separated by scoria. Fifteen of our samples yield ages clustered between 1.36 ± 0.11 and 2.08 ± 0.08 Ma (Table 2). Samples from the Unda-Gamarri, Dobi graben, Isso-Deda’i, and Gamarri blocks are all between 1.1 and 2.1 Ma, i.e., the upper stratoid formation. Similar ages are found south of Siyarrou block. All blocks share essentially the same age ranges. The five samples dated at the Gamarri section (Table 2) [*Kidane et al.*, 1999], further age results by *Lahitte* [2000], and the previous results by *Courtilot et al.* [1984] on the stratoid formation are mostly in the age range of the upper stratoid formation.

[20] The so-called Gulf basalts outcrop mainly along large rhyolitic massifs close to Immino graben, at the northeastern margin of the Manda-Hararo rift system, and

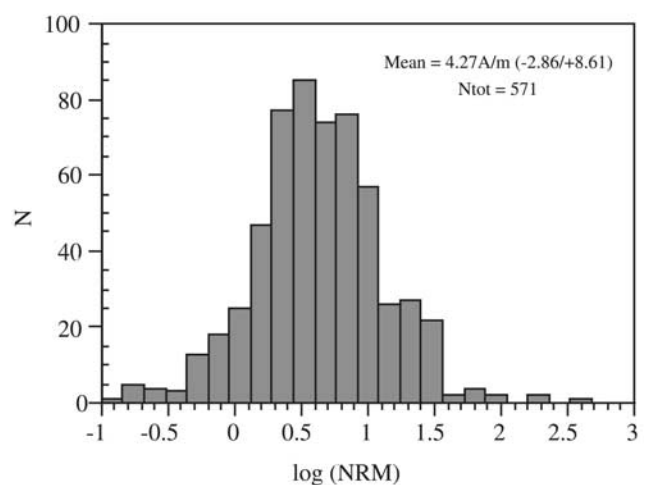


Figure 5. Histogram of 571 measured Natural Remanent Magnetizations (NRM) (number versus decimal logarithm of NRM in A/m) for stratoid samples from this work and the study of *Acton et al.* [2000]. Mean (lognormal) variance and total number of samples are given in the upper right-hand corner.

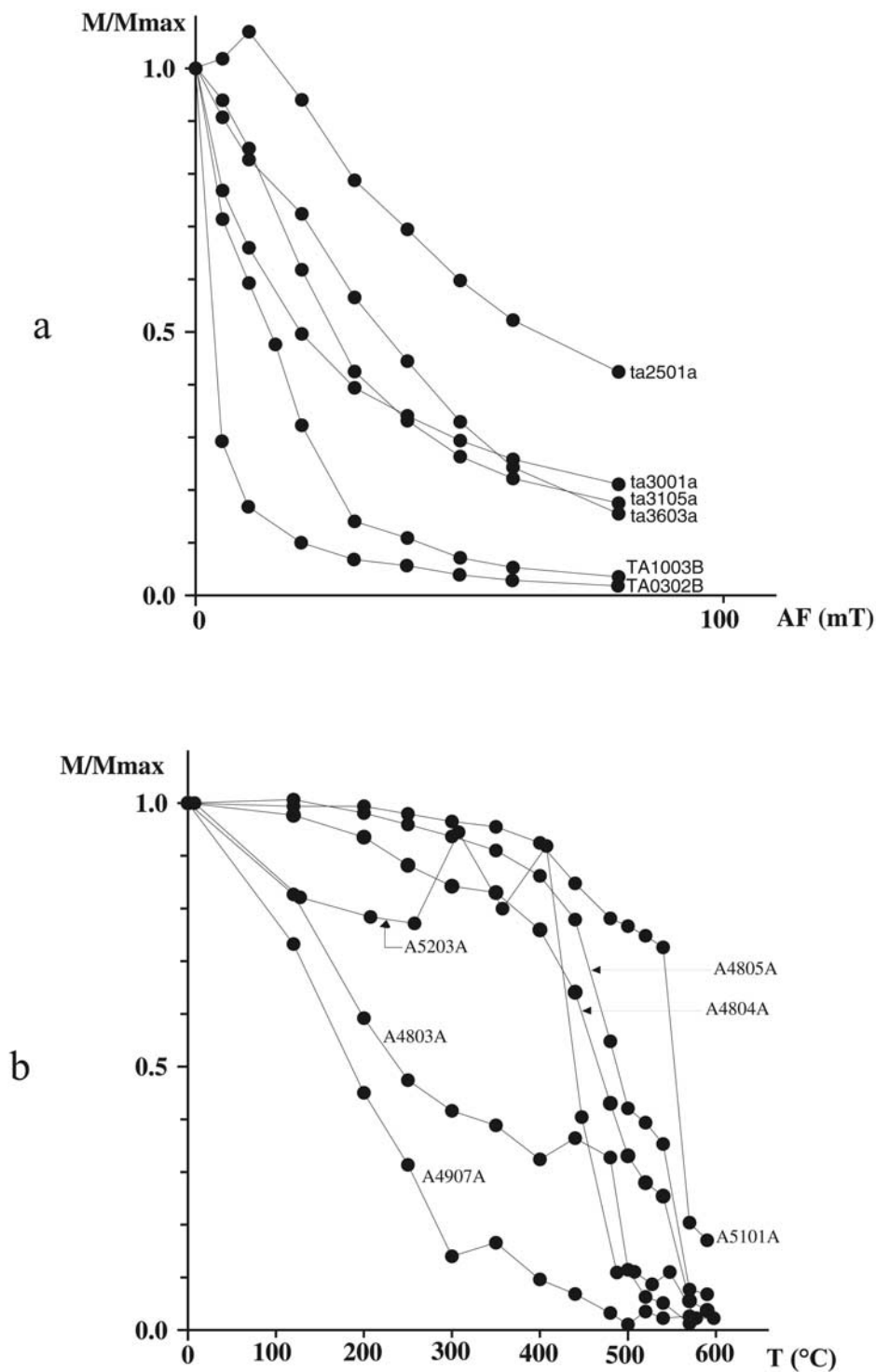


Figure 6. Normalized intensity curves for representative samples demagnetized by (a) AF and (b) thermal treatment. Field in mT and temperature in °C.

in the area close to the Azelo volcano east of Gewane village (Figure 3a). Wherever found, they represent the uppermost chronostratigraphic unit. Exposure is largely surficial and along fault scarps. The ages for this formation range between 0.59 ± 0.16 and 1.11 ± 0.09 Ma. Our samples

were collected from areas previously mapped as part of the “stratoid series” [Varet *et al.*, 1975]. Because of their distinct age, mode of exposure and emplacement, we refer to this as a separate formation, and correlate it with the coeval Gulf basalts mapped elsewhere. Table 2 summarizes

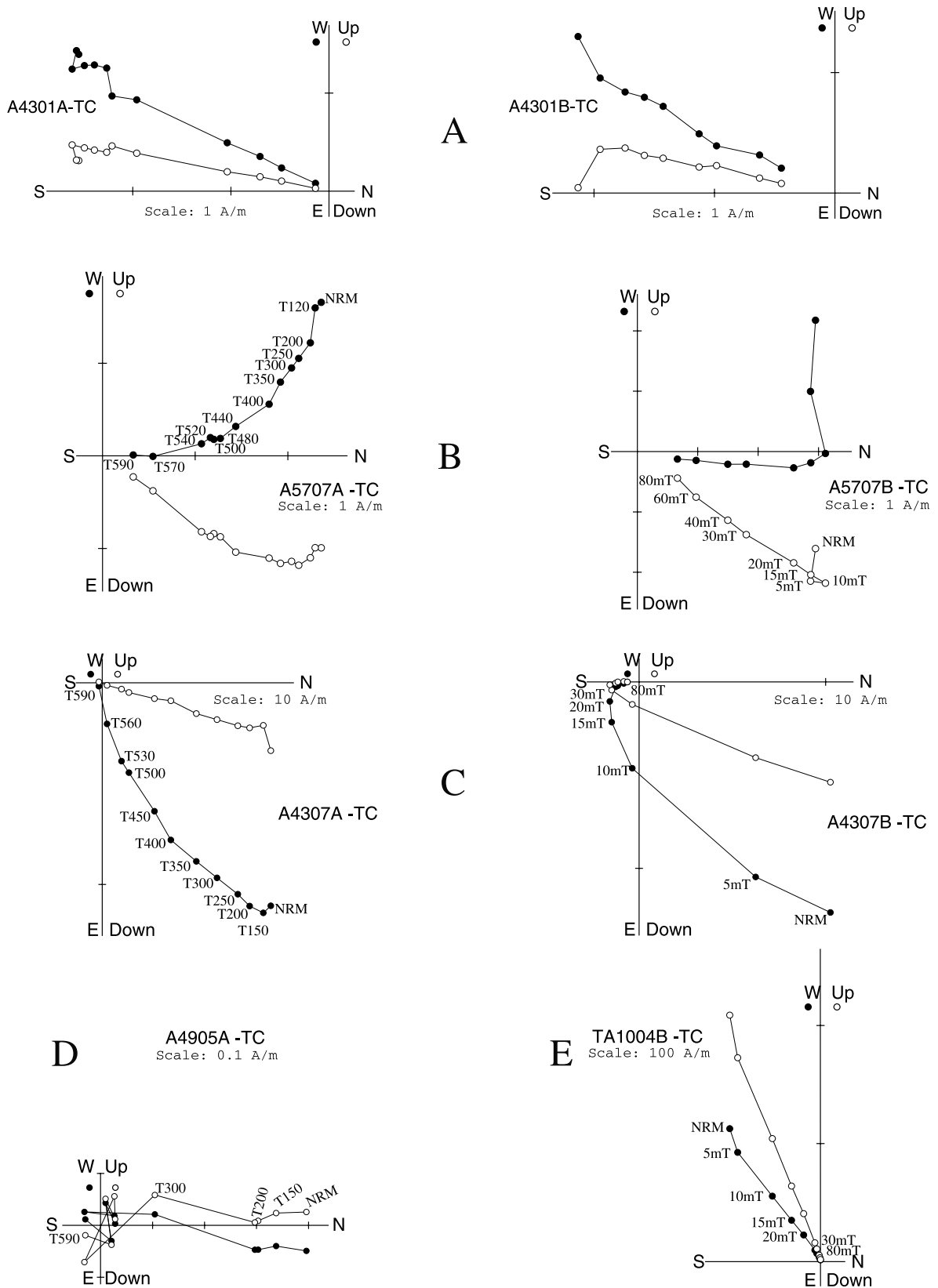


Figure 7. Representative Zijderveld (orthogonal vector) diagrams for samples submitted to thermal (in °C) and AF (in mT) demagnetizations. Categories A, B, C, D, and E are described in the text. Two companion samples demagnetized with both techniques are shown for categories A, B, and C.

Table 3. Mean Paleomagnetic Directions^a

Mile-Gewane Block								
Site	<i>N</i>	<i>D_s</i>	<i>I_s</i>	<i>K_s</i>	(α_{95}) _s	Age, Ma	Formation	
TA05	5	6.4	16.0	27.6	14.8	2.7 ± 0.09	Lower strat.	
TA25	9	168.4	5.4	118.9	4.8	3.3 ± 0.06	Lower strat.	
TA26	7	187.6	-3.5	279.1	3.7		Lower strat.	
TA27	8	192.8	-32.0	142.7	4.7		Lower strat.	
TA28	5	194.9	-35.0	37.5	12.7		Lower strat.	
TA29	5	177.3	-10.7	59.1	10.8		Lower strat.	
TA30	6	183.7	-13.4	92.1	7.0		Lower strat.	
TA37	6	167.6	-16.5	235.0	4.4		Lower strat.	
TA38	6	169.5	-15.6	318.5	3.8		Lower strat.	
TA39	5	183.8	-25.9	126.5	6.8		Lower strat.	
TA40	6	186.2	-24.0	55.4	9.2	3.2 ± 0.19	Lower strat.	
TA03	5	175.6	-23.9	68.0	9.3	1.9 ± 0.07	Upper strat.	
TA04	7	179.2	-17.9	351.4	3.3	2.1 ± 0.08	Upper strat.	
TA23	6	169.4	8.2	153.5	5.4	1.6 ± 0.05	Upper strat.	
(ET37)*	7	180.9	-41.8	81.0	7.4		Upper strat.	
ET38*	5	167.5	-19.6	992.3	2.5		Upper strat.	
(ET39)*	6	167.4	-32.5	57.9	8.9		Upper strat.	
(ET40)*	5	28.1	-49.2	49.2	11.8		Upper strat.	
(ET41)*	5	4.4	43.0	74.4	9.2		Upper strat.	
ET42*	6	345.7	31.5	579.6	2.8		Upper strat.	
TA31	5	17.9	23.8	112.7	7.2	0.7 ± 0.06	Recent bas.	
TA32	7	10.3	21.0	174.0	4.6		Recent bas.	
TA33	6	10.9	28.4	309.7	3.8		Recent bas.	
TA34	6	0.0	29.0	218.2	4.5		Recent bas.	
TA35	5	3.3	26.3	58.3	10.1		Recent bas.	
(TA36)	6	24.3	16.6	128.7	5.9		Recent bas.	
Ali Sabieh Block, South of Hol Hol Fault ^c								
Site	<i>N</i>	<i>D_g</i>	<i>I_g</i>	<i>D_s</i>	<i>I_s</i>	(α_{95}) _s	Age, Ma	Formation
(A18)	7	252.6	-3.6	252.6	-3.6	6.2		Lower strat.
A19	8	2.8	-7.7	2.8	-7.7	3.3		Lower strat.
A20	6	.4	-9.6	.4	-9.6	7.7		Lower strat.
A41	6	177.8	-23.4	177.8	-23.4	4.0		Lower strat.
(A42)	5	200.9	-1.6	200.9	-1.6	9.5		Lower strat.
A43	9	195.9	-6.7	197.4	-7.4	8.0		Lower strat.
A48	7	186.4	-26.1	186.4	-26.1	3.6		Lower strat.
A50	4	180.8	-18.4	180.8	-18.4	10.0		Lower strat.
A51	6	164.9	-9.8	164.9	-9.8	11.0		Lower strat.
(A52)	8	196.7	46.7	196.7	46.7	5.3		Lower strat.
A54	9	179.8	-20.5	(160.0	-49.1)	8.1		Lower strat.
(A01)	9	4.7	-40.7	4.7	-40.7	6.6	1.5 ± 0.05	Upper strat.
(A22)	5	252.2	0.6	252.2	0.6	7.4		Upper strat.
A23	8	4.2	19.1	4.2	19.1	4.3	1.8 ± 0.02	Upper strat.
A55	9	187.0	-41.6	187.0	-41.6	5.5	1.4 ± 0.03	Upper strat.
A53	6	202.9	-35.0	218.3	-30.4	5.3		Recent bas.
(A56)	7	356.2	17.0	356.2	17.0	21.6	0.6 ± 0.02	Recent bas.
A57	9	357.1	29.7	357.1	29.7	6.7		Recent bas.

^aSites between parentheses are not used in calculation of the mean (reasons for removal include too few samples, too large α_{95} , transitional directions, and combination of several flows into a single cooling unit; see text). ET sites are from G. Acton (personal communication, 1998) and *Acton et al.* [2000]; *N*, number of samples; *D*, *I*, declination and inclination in degrees (subscript g for geographic or in situ coordinates, subscript s for tilt-corrected or stratigraphic coordinates). *K* and α_{95} are *Fischer's* [1953] statistical parameters. New K-Ar geochronological measurements are indicated when available (see Tables 1 and 2) and formation name (lower stratoid, upper stratoid, and recent or "Gulf" basalts).

^bReinterpreted sites for which our reinterpretation was significantly different from that of Acton. Otherwise, the *Acton et al.* [2000] values are used.

^cSee Figure 3a and *Audin* [1999].

geochronological results from the present and several earlier studies in the general area of Figures 3b and 3c.

4. Paleomagnetism

4.1. Sampling, Measurement of Remanence, and Treatment

[21] Altogether, 133 sites were sampled for paleomagnetism in the depression. Figure 3c shows where most paleomagnetic sites were collected. Additional sites collected on the Mile-Gewane block to the south of the area of Figure 3c, and near the Ali Sabieh block in southeastern Afar [*Audin*,

1999], are shown in Figure 3a. A "site" was generally a single flow, or 2 flows, though in one case up to 13 flows were sampled. At least 6 and up to 10 cores were drilled at a site, with separation of meters to tens of meters between cores. Standard 2.2 cm long samples were cut from the 2.5 cm diameter cores in the laboratory. All measured samples are reported in the tables, though when the total number of samples was less than 4 data were not used further.

[22] Cores were oriented in the field most of the time with both a solar and a magnetic compass. *Acton et al.* [2000] report a mean deviation of $1.0 \pm 0.4^\circ$ for 368 joint determinations. We added those to our 865 joint determinations: for

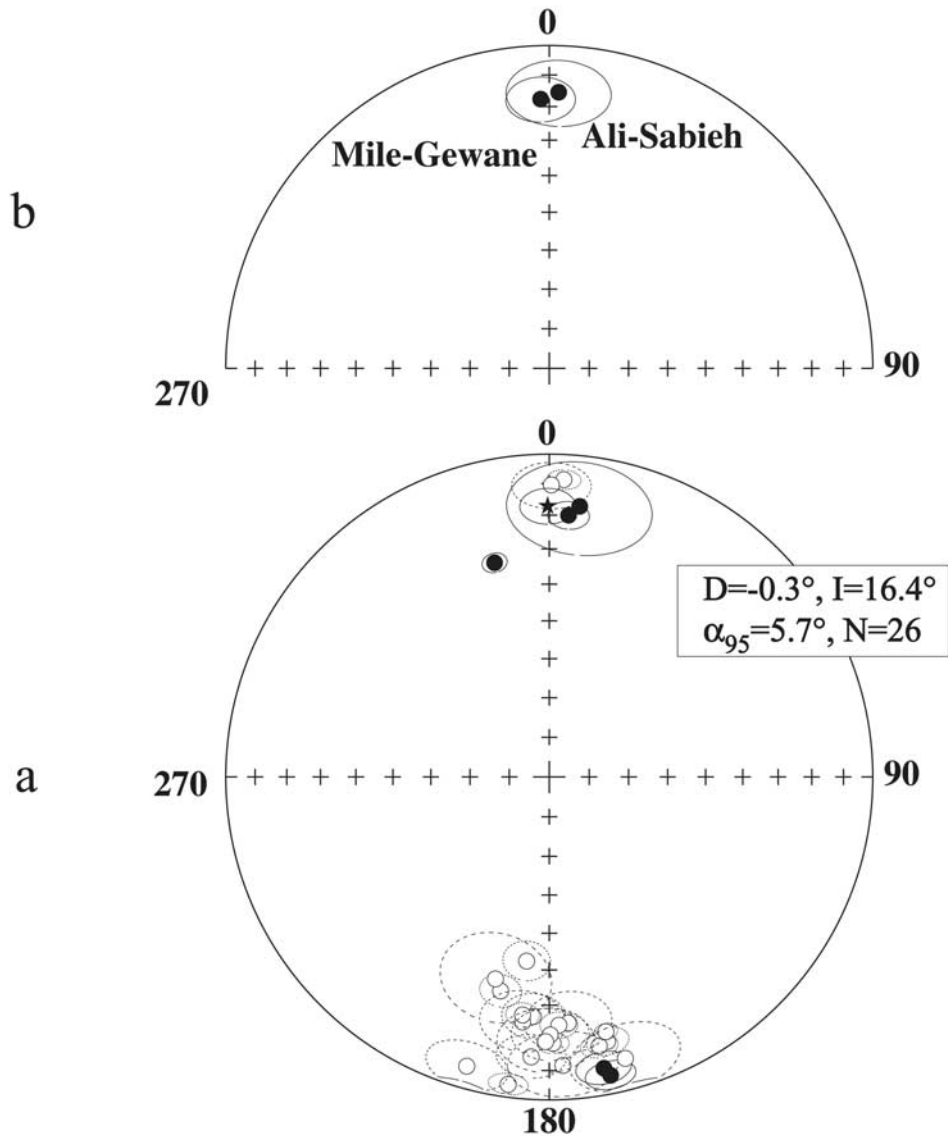


Figure 8. (a) Stereographic projections of characteristic magnetization directions from sites of stratoid series basalts in the Mile-Gewane and Ali-Sabieh blocks (see Figures 2 and 3a) and overall magnetization direction (star) with 95% confidence interval. Mean direction values are given in inset with statistical parameters (26 sites). (b) Comparison of separate averages from sites in the Mile-Gewane and Ali Sabieh blocks, respectively (see Table 3 and text).

these 1233 data, the overall mean difference between azimuths is 1.4° , with a standard deviation of 17.7° and a standard error of 0.5° . When 47 samples with differences larger than 15° are removed, the average becomes 0.7° , the standard deviation 4.0° and the standard error 0.1° . This is in excellent agreement with previous determinations of *Courtillot et al.* [1984] and *Kidane et al.* [1999] and shows that there is no significant systematic magnetic bias.

[23] Magnetizations were measured on either a JR5 spinner magnetometer or a horizontal 2G cryogenic magnetometer, in the shielded room at IPG in Paris. The natural remanent magnetizations (NRM) from 571 stratoid samples (i.e., ours plus those of *Acton et al.* [2000]) are shown in histogram form in Figure 5. The lognormal mean is 4.3 Am^{-1} (2.9/8.6); the distribution displays two modes, a

major one at 3.6 Am^{-1} , and a secondary one at 15.8 Am^{-1} . Such a bimodal distribution has been found for Afar basalts since the study of *Courtillot et al.* [1984] and is interpreted following the study of *Prévot and Grommé* [1975], as indicating that those (minor) basalts with higher magnetizations probably erupted under water, whereas (dominant) basalts with ~ 5 times weaker magnetizations were emplaced subaerially. The high tail of the distribution likely corresponds to basalts struck by lightning.

[24] Samples were demagnetized either by alternating fields in a Schönstedt instrument or thermally in laboratory-built quasi field-free furnaces, or both. Typical demagnetization curves by the two methods are shown in Figure 6. In the case of AF demagnetization, the median destructive field (mdf) is generally between 20 and 35 mT.

Table 4. Mean Paleomagnetic Directions for Recent (Less Than 0.3 Ma) Sites in the Manda-Hararo Rift^a

Site	N	D _g	I _g	D _s	I _s	K _s	(α_{95}) _s
LO10	8	9.5	20.4	9.5	20.7	145.7	4.6
(LO11A)	4	14.3	23.3	14.3	23.3	12.5	27
(LO11B)	4	5.3	30.1	5.3	30.1	93.5	10.1
LO11	8	10.6	26.5	10.6	26.5	22.1	12.1
ET36	8	1.3	11.9	1.3	11.9	90.5	5.9
ET67	7	4.8	24.0	6.3	20.6	249.1	3.8
ET68	6	357.7	13.1	358.5	10.2	434.8	3.2
ET69	7	0.8	16.6	0.8	16.6	473.5	2.8

Fisherian mean: D_s = 4.4°, I_s = 17.8° (α_{95} = 6.4°, N = 6, K = 110.7)
 Bivariate mean: D_s = 4.4°, I_s = 17.8° (α_{95x} = 1.3°, α_{95y} = 6.9°, K_x = 1897, K_y = 68)

^aSites between parentheses are not used in calculation of the mean (see legend of Table 3). Site: site code name; N: number of samples used in statistics; D_g, I_g (D_s, I_s): site mean directions in geographic or in situ and stratigraphic or tilt-corrected coordinates, respectively (only when a significant tilt was measured in the field); K_s, (α_{95})_s, α_{95x} , α_{95y} , K_x, K_y: Fischer [1953] and LeGoff [1990] statistical parameters.

Higher values may correspond to the presence of two components with opposite polarities (ta 2501a in Figure 6a), and smaller ones to samples with very high intensities, most likely struck by lightning (TA1003B and TA0302B in Figure 6a). In the case of thermal demagnetization, most samples have unblocking temperatures between 450°C and 580°C, some with a single or two narrow ranges, and

some with a broader spectrum. Some samples have much lower unblocking temperatures (A4803A and A4907A in Figure 6b): they generally correspond to very weakly magnetized samples, which did not reveal a primary magnetization and carried a jagged secondary overprint (see below and A4905A in Figure 7). For the majority of samples, these diagrams are characteristic of low Ti magnetites, consistent with previous studies of the same formation in other parts of Afar [Courtillot *et al.*, 1984; Kidane *et al.*, 1999; Acton *et al.*, 2000; Manighetti *et al.*, 2001a].

[25] Demagnetization behavior is displayed in vector form in Figure 7. Most samples fall in either one of five distinct categories. Many samples carry a univectorial magnetization, which decays to the origin and is identical under both treatments, sometimes with a very weak overprint that is removed by 200°C or 20 mT (A; Figure 7, sample A4301). In some cases, two distinct components are clearly found, with good separation in AF treatment, but significant overlap in thermal demagnetization (B; Figure 7, sample A5707). Other samples, also with two components, have largely or completely overlapping spectra both upon thermal and AF demagnetization (C; Figure 7, sample A4307). A (small) fourth category, already mentioned above, consists of weakly magnetized samples with a jagged (most likely recent) overprint erased by 300–350°C and erratic behavior above (D; Figure 7, sample

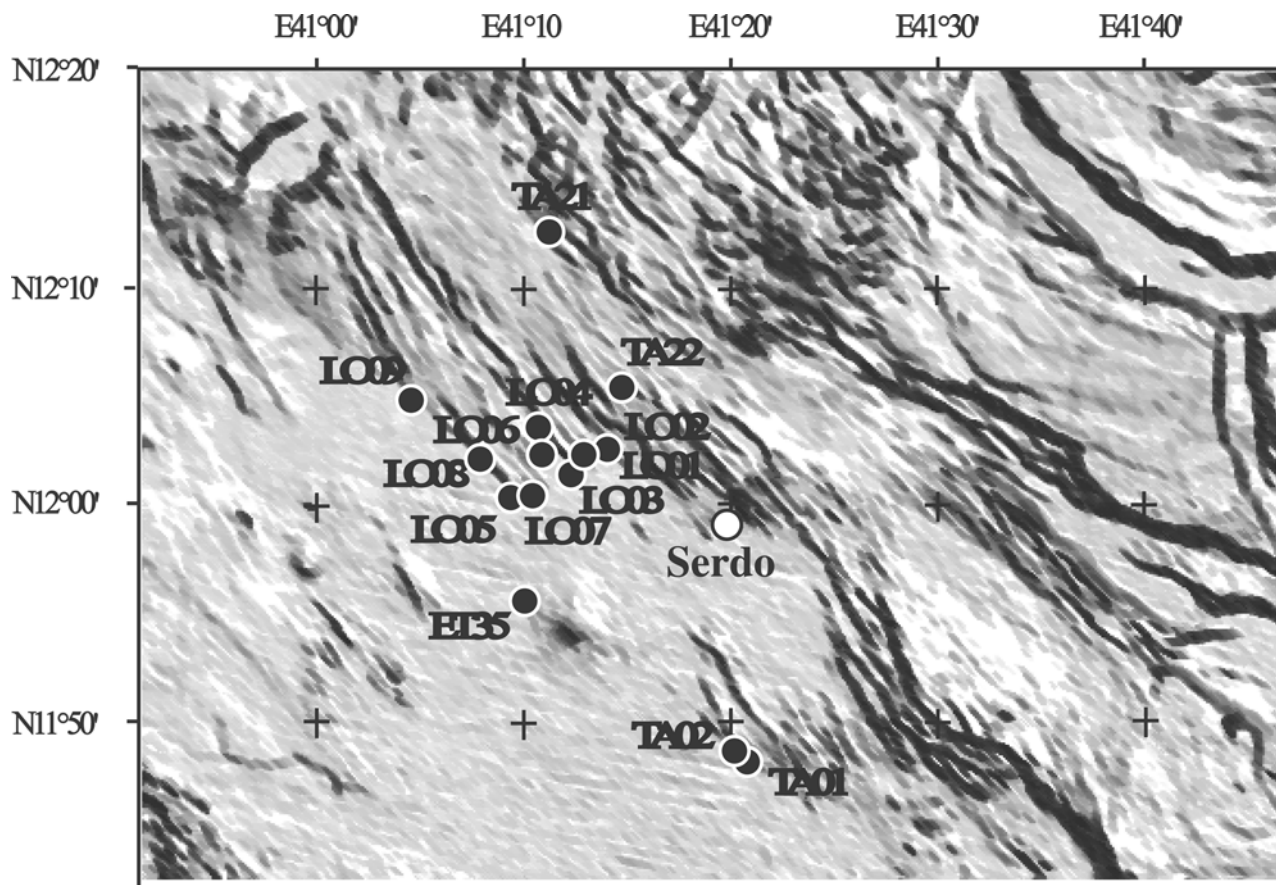


Figure 9. Detailed location of sites in Manda-Hararo rift (see Figures 2 and 3c) with a rough indication of topography.

Table 5. Mean Paleomagnetic Directions for ~0.3 Ma Sites in the Serdo-Semera Microblock (see Table 4)

Site	N	D _g	I _g	D _s	I _s	K _s	(α_{95}) _s
(LO1)	3	209.4	-9.0	209.2	-13.9	133.7	10.7
LO2	4	206.1	-0.9	206.0	-1.5	110.4	8.8
(LO3A)	5	198.7	-9.9	198.4	-15.8	140.5	6.7
(LO3B)	4	204.3	-10.7	204.2	-16.7	342.4	5.0
(LO3C)	3	209.7	-9.2	209.7	-15.2	66.3	17.9
LO3	12	203.6	-10.0	203.5	-16.0	113.5	4.1
(LO4A)	6	204.4	-9.1	204.6	-9.9	210.1	4.8
(LO4B)	6	203.5	-9.7	203.2	-11.1	194.3	5.2
LO4	12	204.1	-9.4	204.0	-10.4	225.4	3.0
(LO5A)	2	16.6	0.8	16.6	0.8	794.8	8.9
(LO5B)	4	6.6	6.3	6.4	9.0	88.0	9.9
LO5	6	9.9	4.5	9.8	6.3	71.9	8.0
(LO6A)	4	202.7	-8.4	202.6	-9.9	187.2	6.7
(LO6B)	4	203.3	-15.7	203.2	-16.4	182.2	7.2
(LO6C)	5	203.6	-7.5	203.5	-10.5	218.4	5.2
(LO6D)	3	197.0	-6.1	197.0	-6.1	230.2	8.1
(LO6E)	2	196.3	3.6	196.3	3.6	1156.4	7.4
LO6A-D	16	202.0	-9.5	202.0	-11.0	144.2	3.1
LO7	5	5.3	17.6	5.3	17.6	97.5	8.0
(LO8A)	4	198.0	12.4	198.0	11.6	1378.8	2.5
(LO8B)	4	201.9	-7.2	201.8	-8.4	108.7	10.3
LO8	8	200.0	4.3	200.0	3.5	48.3	8.2
LO9A	5	3.4	26.1	3.0	27.8	386.8	3.9
(LO9B)	3	14.5	10.8	14.4	13.7	892.7	4.1
(TA01)	5	223.7	30.1	223.7	30.1	90.3	8.3
(TA02)	6	314.8	-43.4	314.8	-43.4	300.3	3.9
(TA24)	6	228.3	41.0	228.3	41.0	297.2	3.9
TA21	4	181.8	-12.9	181.8	-12.9	152.0	8.7
TA22	4	173.1	-4.0	173.1	-4.0	191.1	6.7
ET035	13	351.8	13.4	351.8	13.4	549	1.8
Mean 1 (LO5, LO7, LO9A, TA21, TA22, ET035):				D _s = 0.8°, I _s = 13.7°			
(α_{95} = 9.1°, N = 6, K = 54.8)							
Mean 2 (LO2, LO3, LO4, LO6A-D, LO8):				D _s = 203.1°, I _s = -7.1°			
(α_{95} = 7.8°, N = 5, K = 98.2)							

A4905). Finally, strongly magnetized samples (over several 10^2 Am⁻¹) correspond to lightning (E; Figure 7, sample TA1004B). Most samples fall in the A, B, or C category. In the A and B cases, components were extracted using principal component analysis [Kirschvink, 1980]. In the case of overlapping spectra, the Halls [1976, 1978] remagnetization circles method was used. The two kinds of data were integrated following the study of McFadden and McElhinny [1988]. Low blocking field or temperature components generally average close to the present field direction in Afar and are recent overprints. There is little ambiguity in extracting the more resistant Characteristic Remanent Magnetization (ChRM). As in previous work on Afar basalts, we found that the AF technique was particularly efficient in allowing us to extract the ChRM (Figure 7, A and B categories) and this was used for 90% of the samples.

4.2. Site Mean Paleomagnetic Directions

4.2.1. “Stable” Africa: The Mile-Gewane and Ali Sabieh Blocks

[26] Twenty new sites from the Mile-Gewane “block” (labeled TA) are reported in Table 3. Measured ages range from 0.7 to 3.3 Ma. To these we added six sites (labeled ET) studied by Acton *et al.* [2000] and communicated in detail by Gary Acton (personal communication, 1998). We reinterpreted these data using the same methods and interpretation software as used for the rest of our study (J. P. Cogné, personal communication, 2000). Our reinterpretation gener-

ally led to results similar to those published by Acton *et al.* [2000], though some differences were found [Kidane, 1999]. For instance, most Zijderveld diagrams for samples of site ET37 have widely overlapping unblocking field and temperature spectra, so that 5 out of 7 samples yielded only great circles. As a result, there is a large uncertainty on the average from that site. Three other sites (ET39–41) yield distributions which are far from Fisherian. The data points form an elongate distribution, with “anisotropies” (K_x/K_y ratios, see Le Goff’s [1990] bivariate analysis) ranging from 15 to 150. The four sites, listed in parentheses in Table 3, are therefore excluded from further consideration. Altogether, there are 22 site results available for the Mile-Gewane block.

[27] The separate averages calculated for the upper and lower stratoid series are statistically indistinguishable and can be averaged together yielding a mean direction D = 358.3°, I = 17.3° (α_{95} = 7.1°, N = 16) in stratigraphic coordinates. The remaining six sites of recent basalts come from two separate locations close to the village of Gewane. The distribution of averages is somewhat elongate. The overall mean direction is D = 11.3°, I = 24.4° (α_{95} = 7.9°, N = 6).

[28] Fifty-seven sites were collected in the Aysha-Ali Sabieh region (Figure 3a). Sites from the Dahla basalts (~4.5–7 Ma) and Mabla rhyolites (up to 20 Ma) are reported elsewhere [Kidane, 1999; Audin, 1999] (Audin *et al.*, submitted manuscript, 2002). Eighteen sites of stratoid and recent basalts are reported in Table 3. Most sites provided readily interpretable results, though 6 were eventually eliminated (shown in parentheses). Sites A18, A52, A01, and A22 are remote from the rest of the distribution and may correspond to large local rotations (A18 and A22) or to transitional directions (A52 and A01). Site A56 was eliminated because of its large uncertainty (α_{95} = 22°; all site mean directions with α_{95} larger than 15° were eliminated from calculations of means throughout the paper). Site A42 was also discarded, because the overprint direction could not be eliminated. A tectonic correction was applied in three cases (A43, A54, and A53), but was negligible in two cases. In the case of flow A54, the basalt lies on tilted Jurassic limestones with a 40°SW dip, but application of the tectonic corrections yields an uninterpretable direction, whereas the in situ direction is compatible with other sites: it is likely that flow A54 was emplaced over the already tilted limestones. Its in situ direction is therefore used in calculating the mean. Only two sites are finally available for the upper stratoid formation, and a separate mean could not be determined. Because these two directions were compatible with the population of lower stratoid directions, the 10 available results were averaged, yielding a mean of D = 2.0°, I = 15.1° (α_{95} = 10.6°).

[29] Figure 8b shows that the separate overall means from the Mile-Gewane and Ali-Sabieh blocks are indistinguishable and can be combined. The site mean distribution of the 26 sites (5 with normal polarity and 21 with reversed polarity) is shown in Figure 8a, and the resulting overall mean for “stable” Africa at the time of the stratoid series is D = 359.7°, I = 16.4° (α_{95} = 5.7°). This direction is statistically identical to that predicted for stable Africa at 2 Ma by the synthetic apparent polar wander path of Besse and Courtillot [1991, 2002] (hereafter referred to as BC02). VGP scatter [e.g., Cox, 1969] is 11.6° (9.8° < σ < 17.8°), compatible with

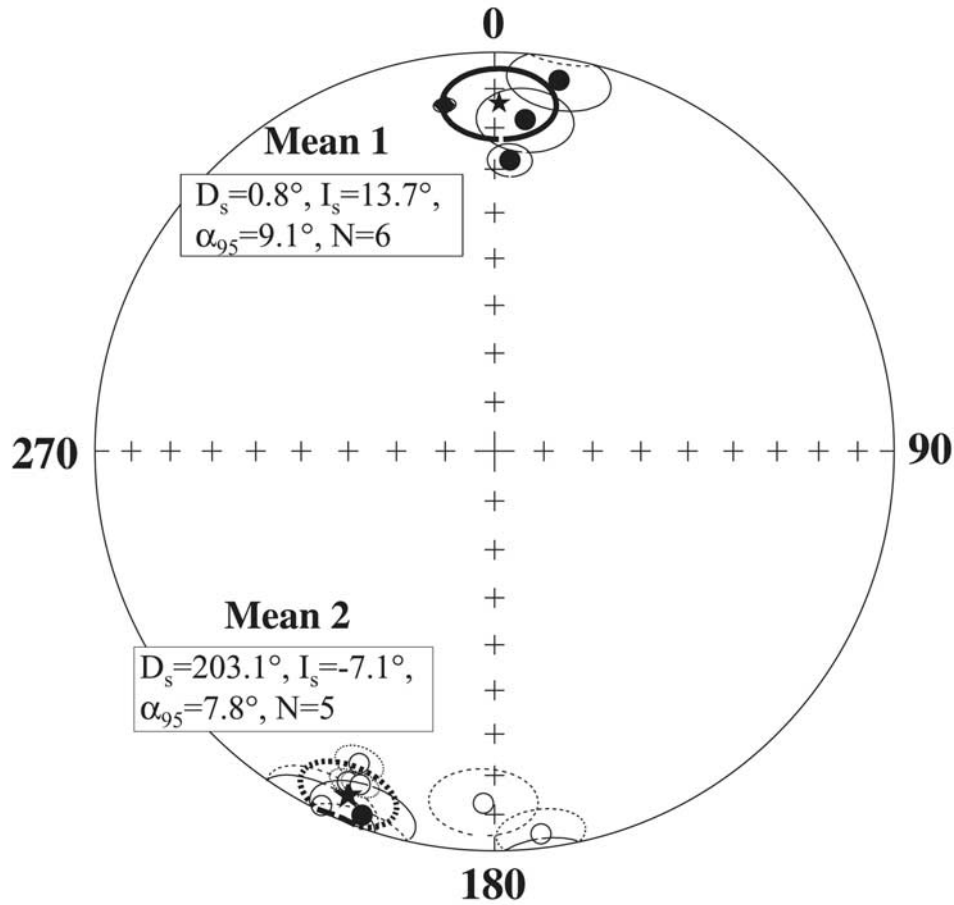


Figure 10. Stereographic projections of characteristic magnetization directions from sites of stratoid series basalts in the Serdo-Semera block (see Figures 2 and 3c) and mean magnetization directions (stars with 95% confidence intervals) for two separate (rotated and nonrotated) subsets (see text). Mean direction values are given in insets with statistical parameters (5 and 6 sites, respectively) (see Table 5).

the prediction of the *McFadden et al.* [1991] model, suggesting that secular variation has been properly recorded.

[30] The 5 sites of “Gulf” basalts from the Mile-Gewane side and the two sites from the Ali-Sabieh side can be combined to yield a mean direction of $D = 6.7^\circ$, $I = 27.0^\circ$ ($\alpha_{95} = 5.4^\circ$, $N = 7$). The slight declination difference ($\Delta D = 6.1 \pm 5.6^\circ$), and inclination anomaly ($\Delta I = 6.0 \pm 5.9^\circ$) with respect to expected values at 0.5 Ma should not be over-interpreted, due to the small number of sites.

4.2.2. The Manda-Hararo Rift

[31] We next describe paleomagnetic results from individual blocks in the order they are encountered along the road going from the Ethiopian rift northward. For the sake of completeness, we briefly report three sites that were sampled on the young (<0.3 Ma) axis of the Manda-Hararo rift (Table 4). Two superimposed flows from the same site actually yield statistically identical directions (due to the large α_{95} of L011A), which can therefore be combined as a possibly single cooling unit. Our two independent results (L010 and 11) can then be combined with four sites from the study of *Acton et al.* [2000]. The mean lies at $D = 4.4^\circ$, $I = 17.8^\circ$ ($\alpha_{95} = 6.4^\circ$, $N = 6$), which includes the present field direction ($D = 0^\circ$, $I = 22^\circ$). However, the distribution is quite elongated and a bivariate analysis yields an

Table 6. Mean Paleomagnetic Directions for ~1.8 Ma Sites in the Unda-Gamarri Microblock (see Table 4)

Site	N	D _g	I _g	D _s	I _s	K _s	α_{95s}
(TA06)	5	170.1	13.8	170.1	13.8	98.5	7.7
(TA07)	5	175.1	11.7	175.1	11.7	115.6	7.1
TA06-07	10	172.6	12.8	172.6	12.8	104.9	4.7
TA08	5	180.1	-18.9	180.1	-18.9	514.8	3.4
TA09	5	178.2	-20.7	179.5	-21.2	135.5	6.8
TA15	6	195.7	-22.8	195.7	-22.8	532.3	2.9
TA16	5	186.7	-32.6	186.7	-32.6	42.7	12.2
TA17	5	173.6	-0.6	173.8	-0.6	54.8	10.4
TA18	5	189.3	-31.7	189.2	-31.8	135.7	6.8
TA19	6	166.8	-21.9	166.8	-21.9	113.2	7.1
TA20	5	191.0	-24.6	191.0	-24.6	389.7	4.2
ET06	6	183.3	-23.0	188.3	-15.5	84.7	7.3
ET08	6	180.4	-38.2	190.2	-30.8	613.3	2.7
ET09-12	22	160.1	-11.7	163.1	-9.9	56.6	4.2
ET13	5	173.8	-13.3	176.8	-8.5	62.7	9.7
ET14-15	17	343.3	45.2	358.2	41.6	27.7	6.9
ET16	6	351.7	6.8	353.0	2.8	284.5	4.0
ET18	8	179.3	-8.2	179.3	-8.2	425.9	2.7
ET19-20	15	180.7	-20.5	180.7	-20.5	220.6	2.6
Mean:		D _s = 0.0°	I _s = 17.9°	($\alpha_{95} = 7.1^\circ$, N = 17, K _s = 25.9)			

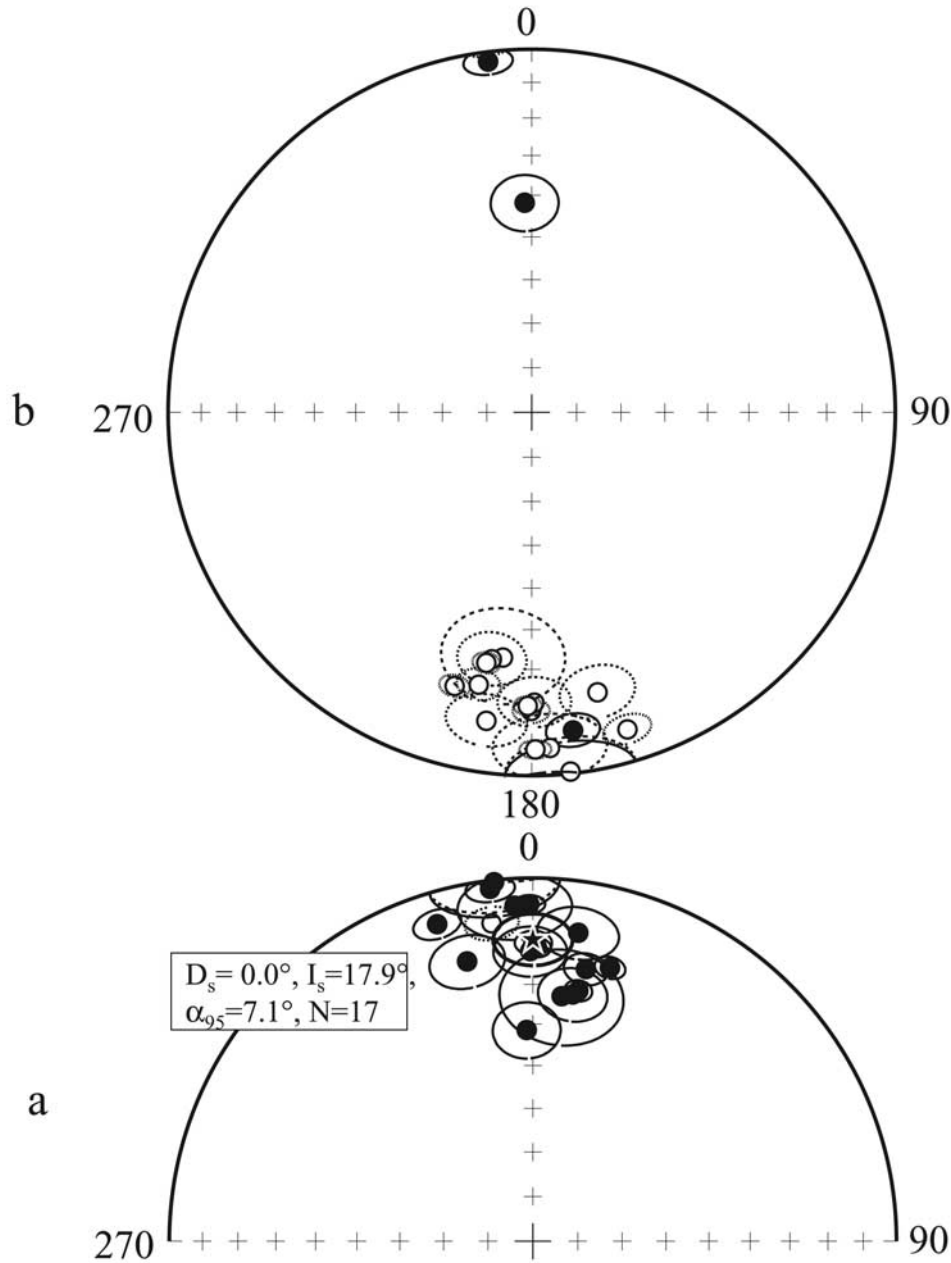


Figure 11. (a) Stereographic projections of characteristic magnetization directions (all flipped to normal polarity) from sites of stratoid series basalts in the Unda-Gamarri block (see Figures 2 and 3c) and mean magnetization direction (star with 95% confidence interval). Mean direction values are given in inset with statistical parameters (17 sites). (b) Individual site mean directions with original polarities (see Table 6).

“anisotropy” ratio in excess of 5. We have no explanation for this feature. Our results are not incompatible with the idea that the Manda-Hararo rift has not been subjected to significant recent rotations.

4.2.3. The Serdo-Semera Block

[32] This block comprises a slightly older part of the Manda-Hararo rift, made of “Gulf” basalts dated between 0.6 and 1.1 Ma. We have sampled 24 flows and one site comes from *Acton et al.* [2000] (ET35). Figure 9 shows site locations in their tectonic context and Table 5 lists the characteristic directions for each flow. In a number of cases, overlying flows from a similar location gave indis-

tinguishable directions and could be merged as single cooling units (L03, L04, L05, and L06). In cases where less than three specimens could be determined, the average was not retained. In three cases, directions were clearly transitional in nature (or strong overprints had not been removed) with intensities 10 times less than average (TA01, TA02, TA24; Figures 3c and 9). This is unfortunate, since these flows were located at the southern-faulted edge and in the central part of the block, and significantly extended coverage.

[33] The mean directions from the 11 usable sites are spread over a wide range of declinations (Figure 10). On

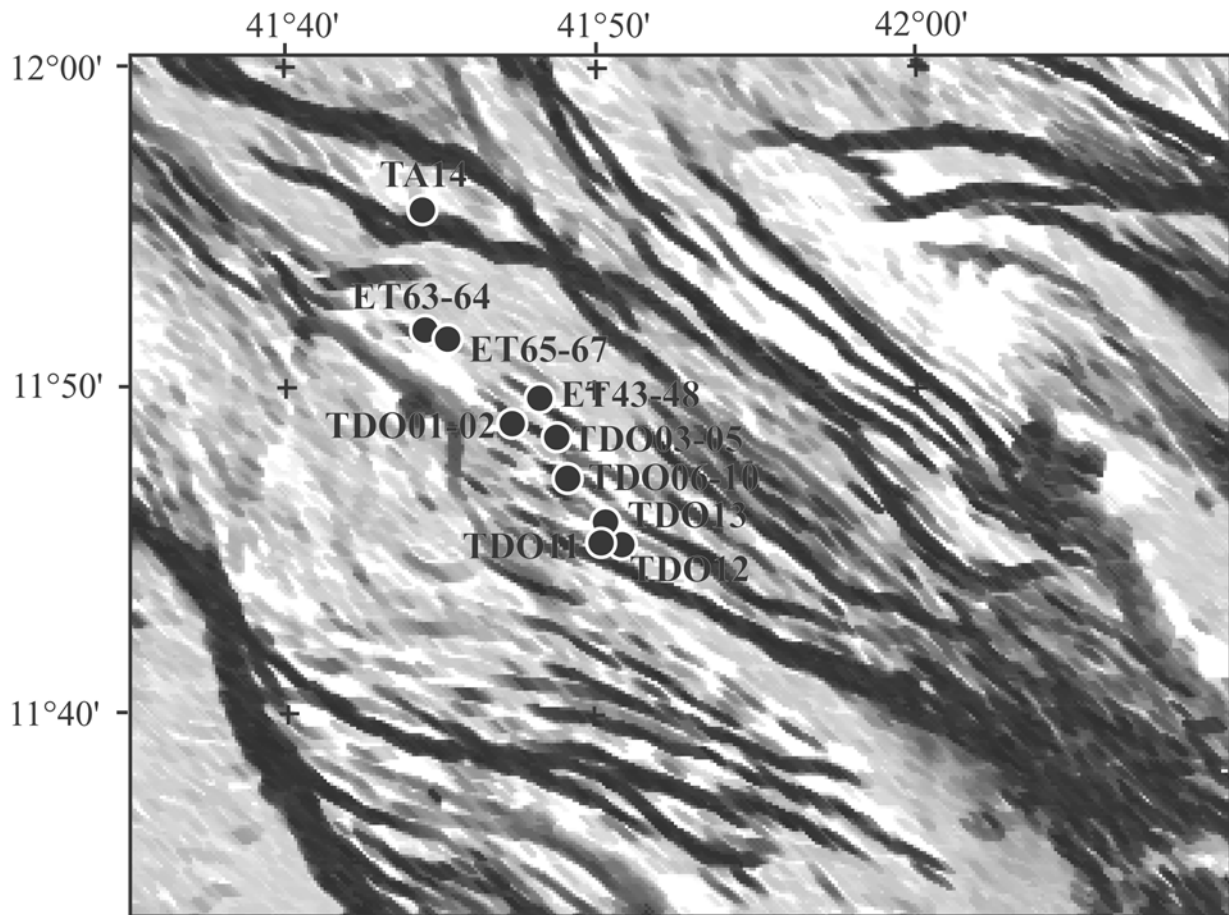


Figure 12. Detailed location of sites in Dobi block (see Figures 2 and 3c) with a rough indication of topography.

closer inspection, two distinct data groups are identified, one with no significant rotation ($D = 0.8^\circ$, $I = 13.7^\circ$; $\alpha_{95} = 9.1^\circ$, $N = 6$), the other with a significant one ($D = 203.1^\circ$, $I = -7.1^\circ$; $\alpha_{95} = 7.8^\circ$, $N = 5$). Yet, the significance of these two groups is quite different. The nonrotated group has both polarities, and forms the external, widest part of the site cluster (Figure 9). On the other hand, the rotated group lies in a small region at the center and has only reversed polarities: ages between 0.8 and 1.0 Ma are consistent with eruption in the Matuyama Chron. The rotation of the central part of this former rift is therefore of local significance only, and the rest of the data are representative of the ~ 1 Ma nonrotated block.

4.2.4. The Unda-Gamarri Block

[34] We sampled 10 sites in order to complement the 15 already sampled by *Acton et al.* [2000]. All belong to the upper stratoid formation (between 1.4 and 2 Ma), except for two (TA17 and TA18) which are younger (1.1 Ma). Mean directions for our data and for those of *Acton et al.* are statistically identical and can be combined (Table 6). Two sites from the *Acton et al.* [2000] study have 95% uncertainties larger than 15° and have been discarded. If we further combine superimposed flows which are likely part of the same cooling unit (TA06–07, ET09–12, ET14–15, and ET19–20), we end up with a Fisherian distribution (Figure 11) with 17 mean directions (2 normal and the rest reversed). The overall average is $D = 0.0^\circ$, $I = 17.9^\circ$ ($\alpha_{95} =$

7.1°), with a positive reversal test. The two sites with slightly younger ages are indistinguishable from the rest. The overall mean is in agreement with the direction expected for stable Africa at 2 Ma ($\Delta D = -2.4 \pm 8.0^\circ$; $\Delta I = -0.1 \pm 7.7^\circ$). VGP scatter for the 17 sites is 11.4° , also in agreement with expected values [*McFadden et al.*, 1991]. The Unda-Gamarri block has therefore not been significantly deformed internally and has not suffered significant rotation since emplacement of the stratoid series.

4.2.5. The Dobi Block

[35] The southern part of the Dobi graben is largely covered by recent sediments, including evaporites. It is densely faulted with $N110 \pm 15^\circ E$ trending normal faults, and lava flows are tilted $15 \pm 5^\circ$ toward $N15^\circ E$. We have collected 13 sites (TDO01–13) in this area (Figure 12), which is part of GATZ. Thirteen sites from the study of *Acton et al.* [2000] are available slightly to the north, to which we added one site even further north (TA14); all are outside of GATZ. Four age determinations within this block range from 1.8 to 2.2 Ma, confirming that the upper stratoid formation covers most of the block.

[36] Paleomagnetic results are given in Table 7. Two sites with strong inclinations have reasonable VGP latitudes in stratigraphic coordinates and are therefore considered as full polarity results, whereas TDO07 with a -59° VGP latitude is considered as transitional and is not included in the mean.

Table 7. Mean Paleomagnetic Directions for ~2 Ma Sites in the Dobi Microblock (see Table 4)

Site	N	D _g	I _g	D _s	I _s	K	α _{95s}
TDO01	5	171.6	-62.8	179.0	-48.6	31.5	14.2
TDO02	6	357.7	16.3	358.4	1.9	122.7	6.3
(TDO03)	5	345.2	38.2	349.5	24.9	23.0	16.3
TDO04	6	4.7	28.8	5.7	14.1	82.6	7.4
TDO05	7	9.0	15.8	9.2	0.9	142.5	5.1
TDO06	5	166.5	-31.6	169.7	-18.2	57.0	10.2
(TDO07)	6	198.5	9.9	198.8	24.9	69.2	8.1
(TDO08)	6	18.3	20.9	18.1	5.9	27.6	13.0
(TDO09)	6	10.0	11.3	10.0	-3.6	92.8	7.0
TDO08-09	11	12.0	14.7	12.1	-0.3	53.7	6.3
TDO10	6	1.1	9.8	1.2	-4.7	118.3	6.2
TDO11	5	335.1	63.9	348.1	51.2	40.0	12.2
(TDO12)	7	3.4	28.5	4.5	13.8	124.6	5.6
(TDO13)	5	357.3	21.1	358.4	6.8	36.5	12.8
TDO12-13	13	1.2	21.8	2.1	7.2	28.3	8.0
Mean A	9	359.8	29.5	1.3	15.0		14.5
TA14	6	0.4	7.5	358.5	29.6	219.3	4.5
ET043	5	190.6	-38.8	198.0	-22.9	116.9	7.1
ET044	4	173.1	-15.8	176.2	-4.9	230.3	6.1
ET045-46	10	184.8	-30.6	190.9	-16.2	686.4	1.8
ET047	6	181.4	7.0	177.6	19.3	288.0	4.0
ET048	6	176.2	-11.9	178.0	-0.3	43.3	10.3
ET049-51	16	165.9	-22.3	171.7	-13.2	345.9	2.0
ET063	6	357.8	39.2	356.7	18.3	175.6	5.1
ET064	8	358.7	31.5	357.8	10.6	583.2	2.3
ET066	5	2.5	37.0	0.7	16.3	160.9	6.1
ET067	7	4.8	24.0	6.3	20.6	249.1	3.8
Mean B	11	359.4	23.1	1.0	12.4		8.6
Mean (A + B):		D _g = 359.6°, I _g = 25.9° (α ₉₅ = 7.7°, N = 20, K _g = 19.1)					
		D _s = 1.1°, I _s = 13.5° (α ₉₅ = 7.4°, N = 20, K _s = 20.3)					

Superimposed flows TDO08-09, TDO12-13, and ET045-46 are considered part of the same cooling units and are therefore averaged. The separate means for our 9 distinct cooling units to the south (within GATZ), and those of *Acton et al.* [2000] plus our site TA14 to the north (outside GATZ) are statistically identical and are therefore averaged together. The result for 20 cooling units from 10 geographically distinct locations is D_s = 1.1°, I_s = 13.5° (α₉₅ = 7.4°) in stratigraphic coordinates (Figure 13 and Table 7). We note that because all flows have similar tilts, there is no conclusive fold test. However, the tilt corrected mean direction is consistent with the expected 2 Ma direction, with ΔD = -1.3 ± 7.8°, ΔI = -4.5 ± 7.9°, and the Dobi block appears to be nonrotated. VGP scatter (12.3° + 4.8/-2.8) is in agreement with the value expected from secular variation.

4.2.6. The Isso-Deda'i Block

[37] The coverage of this block by paleomagnetic samples is quite restricted, since all we have is two short magnetostratigraphic sections only a half kilometer apart. One section comprising 13 superimposed flows is from the study of *Acton et al.* [2000], whereas we have sampled 6 flows, along the same large fault escarpment at a slightly lower altitude. Two age determinations from the lowest and topmost flow in our section (1.93 and 1.76 Ma) are consistent with stratigraphic order and confirm that the upper stratoid series was sampled. The four lower flows have normal polarity and the topmost one is reversed (Figure 14a). Behavior of samples from flow 15 is more complex. Two samples have directions that could clearly be determined, one (TDO15-01A) being very close to the direction

of the overlying reversed flow (TDO14), the other (TDO15-03A) close to that of the underlying flow (TDO16, see Figure 14b). All other samples show AF demagnetizations following great circles and converging either to one or the other direction (Figure 14c). Such behavior in flows coeval with a reversal, or remagnetized shortly after one, is discussed by *Valet et al.* [1998]. These directions were excluded from calculations of site averages.

[38] Interestingly, *Acton et al.* [2000] have captured the same reversal, with their highest flow (ET22) being fully reversed, and the bottom one (ET34) normal. Directions from these 13 flows (Figure 15) in fact streak along a great circle linking the two full polarity directions, and hence the distribution is not Fisherian. Site ET24 has a transitional VGP latitude and was excluded from the mean. Some of *Acton et al.*'s [2000] directions (ET23 and ET26) likely still comprise unseparated overlapping components and are affected by some amount of remagnetization.

[39] Despite this, the mean directions from the two sections are very similar and can be averaged, yielding a mean for 13 cooling units at D = 9.4°, I = 15.7° (α₉₅ = 9.4°) (Figure 16 and Table 8). Because in part of a rather large uncertainty, differences with the 2 Ma reference direction from stable Africa are not significant (ΔD = 6.9 ± 10.1° and ΔI = -3.3 ± 9.8°); VGP scatter is typical of secular variation (9.4° < σ = 11.9° < 16°). The normal to reversed polarity reversal, which has been captured in both sections, is the upper Olduvai termination.

4.2.7. The Siyarrou Block

[40] This block was sampled by *Manighetti* [1993] and *Manighetti et al.* [2001a] in a helicopter trip along the border between Ethiopia and the Republic of Djibouti (Figure 17; I sites). This is now complemented to the west, along the main road, by two sites from the study of *Acton et al.* [2000] and three from our study. Three of our sites (TA10-12) are dated around 0.9 Ma and therefore belong to the recent (Gulf) basalts, whereas all the rest are likely part of the upper stratoid series (TA13 at 1.77 Ma).

[41] *Manighetti* [1993] noted that several of her directions were statistically identical (Table 9, I sites) and that the same up-faulted and down-faulted flow had probably been sampled several times along the helicopter section. We retained 7 directions as corresponding to distinct cooling units, and averaged I25, 27-29 and 32 as a single one. Only 3 samples could be used in flow TA13, whose direction was therefore not included in the mean. Altogether, we obtain 8 independent directions for the upper stratoid series, with a mean (Figure 18a) at D = 5.7°, I = 6.8° (α₉₅ = 12.8°). The uncertainty is unfortunately large and precludes determination of a significant rotation (ΔD = 3.2 ± 13.2°). There may be an inclination anomaly (ΔI = -12.2 ± 13.1°), but this is not significant at the 95% confidence level. VGP scatter, at 10.7°, is in the expected range.

[42] The four "recent" basalts yield a mean (Figure 18b) at D = 357.5°, I = 12.2° (α₉₅ = 12.9°) which is similar to the expected direction at 0.9 Ma.

4.2.8. The Zone North of Immino Graben

[43] There is no apparent structure in the area north of the Immino graben, going all the way up north to the currently active Manda-Inakir rift. This is therefore treated as a single "block." We have not sampled new sites in this zone, but we already have 20 sites from earlier studies in

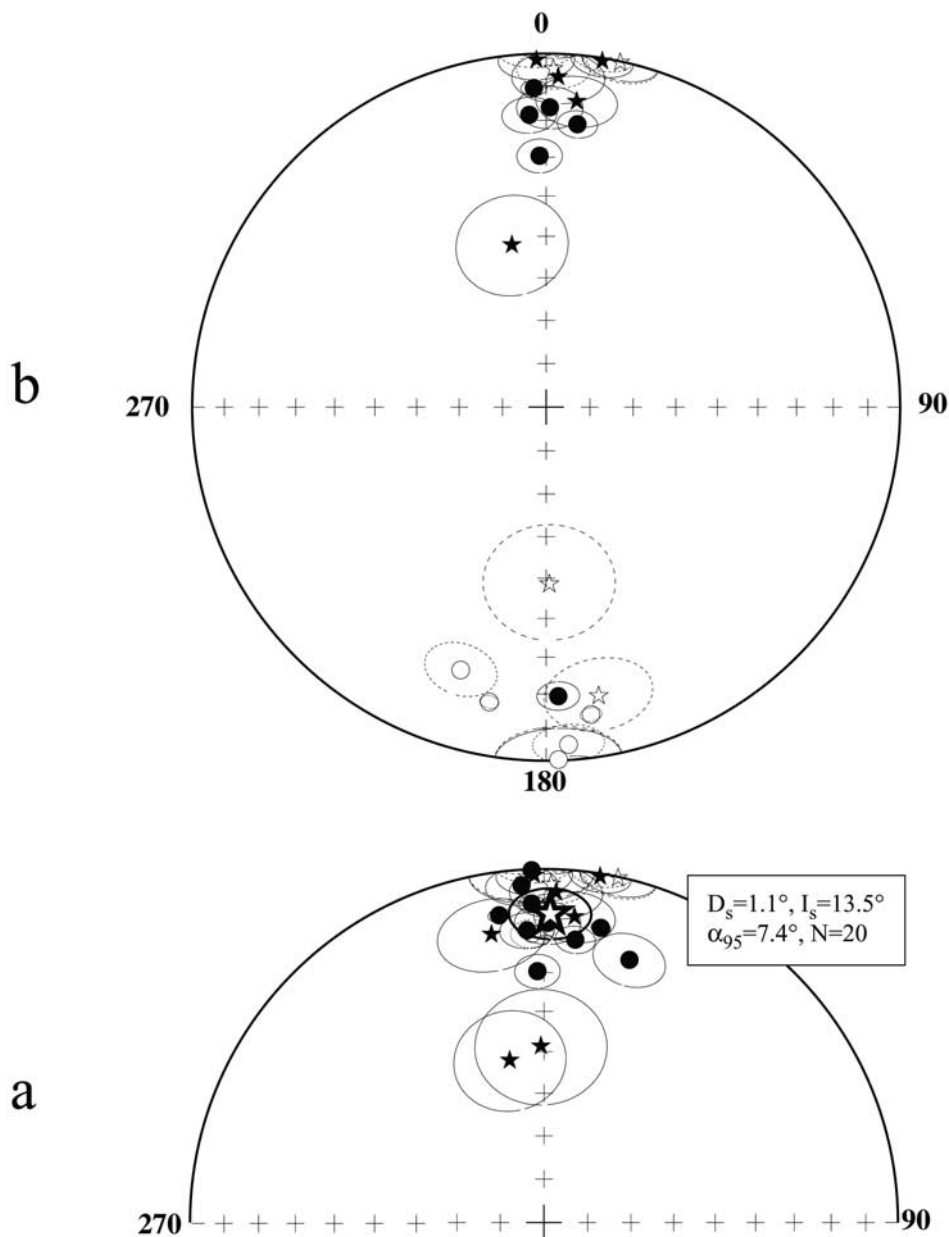


Figure 13. (a) Stereographic projections of characteristic magnetization directions (all flipped to normal polarity) from sites of stratoid series basalts in the Dobi block (see Figures 2 and 3c) and mean magnetization direction (large star with 95% confidence interval). Mean direction values are given in inset with statistical parameters (20 sites). (b) Individual site mean directions with original polarities (see Table 7). Small stars are southern Dobi sites, and circles are northern ones; the two groups are discussed in the text.

Djiboutian Afar [Courtilot *et al.*, 1984; Manighetti, 1993] which can be combined with 9 sites in Ethiopian Afar from the study of Acton *et al.* [2000]. There are only recent (“Gulf”) basalts outcropping. A number of flows, which had similar directions, were coupled into independent cooling units (ET54–58; I02-1, I02-2; I04-1, I04-2). All 17 remaining directions are in agreement (Table 10 and Figure 19) and a single Fisherian average is obtained with $D = 356.4^\circ$, $I = 22.6^\circ$ ($\alpha_{95} = 4.3^\circ$). This is the

direction expected at ~ 1 Ma and there is therefore no significant rotation since emplacement.

5. Ages Versus Magnetic Polarity

[44] The magnetic polarity of all our dated sites is given next to the age values in Table 1 and these are represented in Figure 20 (see also Table 11) as a function of time, along with the Geomagnetic Polarity Timescale (GPTS) of

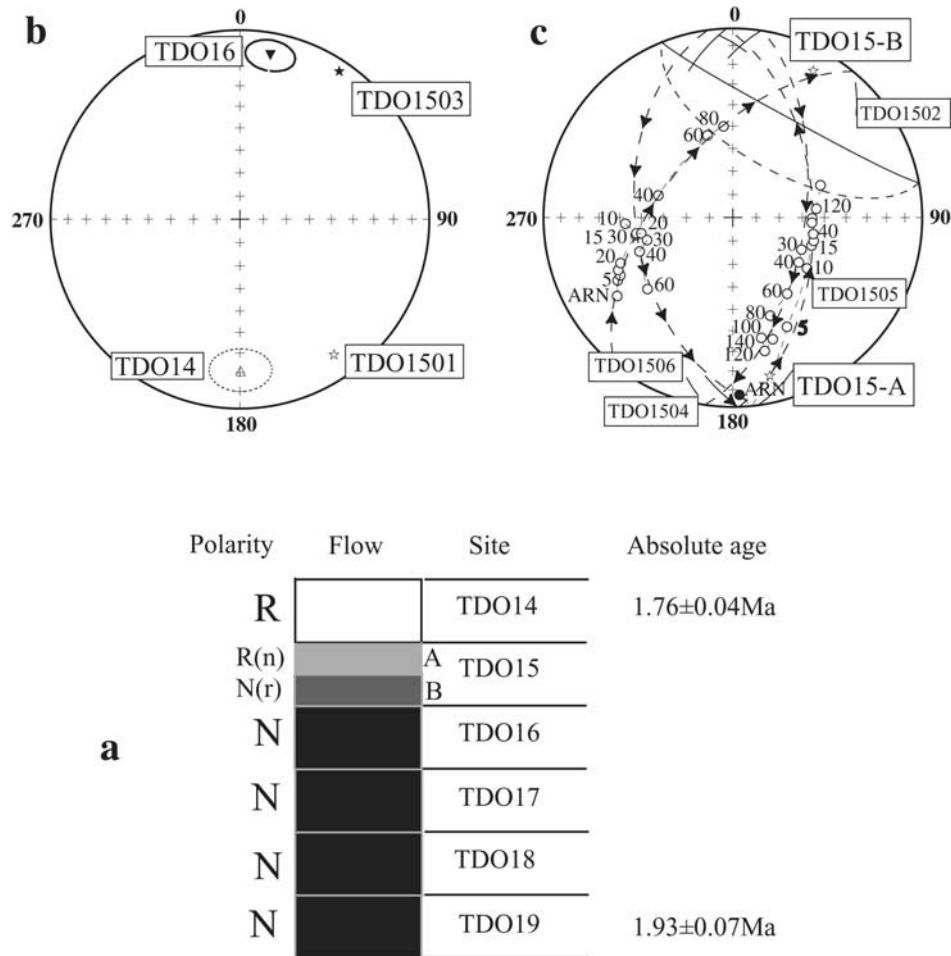


Figure 14. Paleomagnetic results from a series of 6 successive flows on the southern edge of the Isso-Deda'i block (see Figures 2 and 3c). (a) Magnetostratigraphic sequence with flow codes, magnetic polarity, and two absolute age determinations. Flow TDO15 has a complex behavior, which could be interpreted in terms of two partly remagnetized flows. (b) Stereographic projections of mean characteristic magnetization directions for flows TDO16 (normal) and TDO14 (reversed) and directions for individual samples TDO15-01 and TDO15-03 from intermediate flow TDO15 close to TDO14 and TDO16, respectively. (c) Demagnetization paths, roughly along great circles, of samples TDO15-02 and TDO15-06, converging toward the direction of TDO16 and TDO15-03 (subflow TDO15-B?) and similarly TDO15-04 and TDO15-05 converging toward TDO14 and TDO15-01 (subflow TDO15-A?).

Cande and Kent [1995]. Thirty-two out of 36 age determinations have uncertainties less than 150 kyr (at the 1 – σ level) and are in agreement with the polarity predicted from the GPTS. Out of the four remaining data, two have a polarity which agrees with the GPTS, given their larger uncertainty: 70N is normal and is compatible with being in the Jaramillo subchron and 70L (with a 1 – σ uncertainty of 26%) is likely in the uppermost reversed part of the Matuyama chron. The strong atmospheric argon contamination in 70J (Table 1) leads to an uncertainty of 27%. Despite this large value, this reverse sample barely misses the Brunhes-Matuyama transition (but does include it at the 2σ level). With its strong intensity (6.9 A/m), 70J is unlikely to be transitional and could be well within the uppermost reversed part of Matuyama. Sample 72B (paleomagnetic sample TA01) is transitional, yet its 1 – σ uncertainty range is entirely within the Brunhes chron.

Though TA01 seems to be transitional tending on the reversed side, the overlying flow TA02 (not dated) sampled 1 km further north is also transitional but rather tending on the normal side. Both have a magnetization 10 times less than average for Afar basalts with full polarity. 72B could also correspond to one of the events within the Brunhes which have been identified between 550 and 750 ka [Champion et al., 1998; Guyodo and Valet, 1996; Quidelleur and Courtillot, 1996]. The Réunion event was sampled in detail in the Gamarri section [Kidane et al., 1999] and the upper termination of Olduvai (Olduvai/Matuyama transition) was sampled both by us and by Acton et al. [2000]. Samples with age uncertainties less than, say, 50 kyr (there are 8 in Table 2) could be used as constraints in a future reassessment of the GPTS. Of particular interest are samples which could allow better constraints on the ages of the upper Olduvai/Matuyama (72N, 72M, and 75AJ1), lower Olduvai/

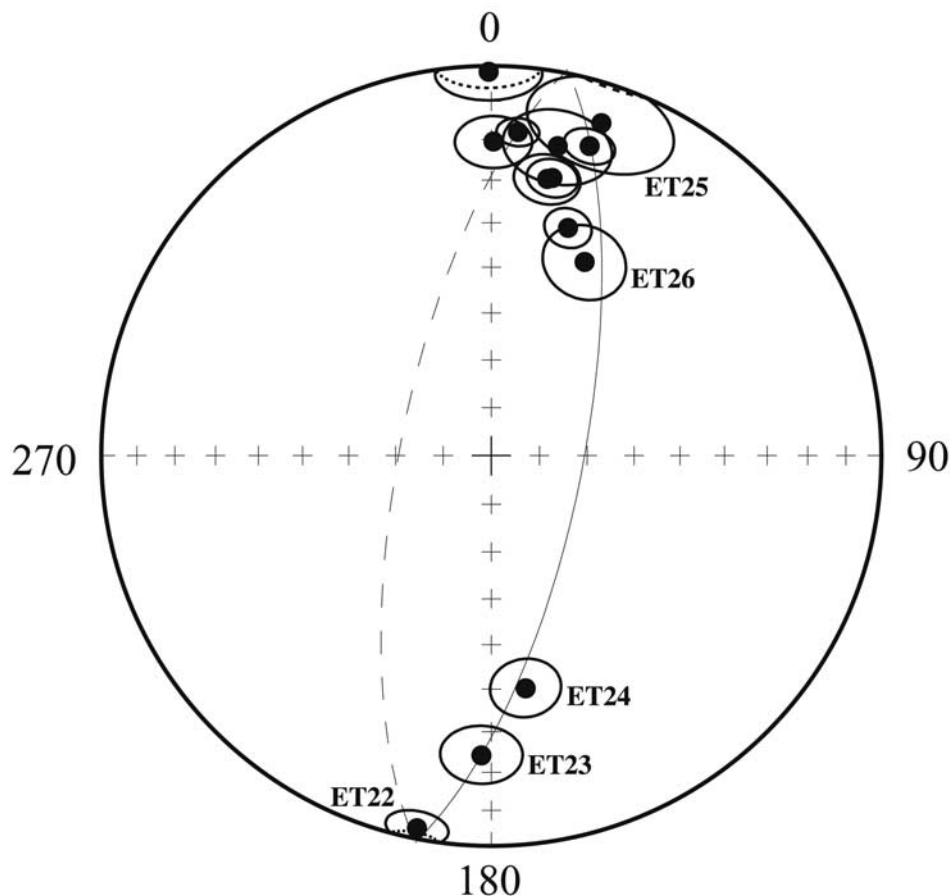


Figure 15. Characteristic directions from 13 superimposed flows, measured by *Acton et al.* [2000] from a section on the southern edge of the Isso-Deda'i block, streak along a great circle, similar to behavior observed in Figures 14b and 14c.

Matuyama (75D and 72O), Reunion (GA02, GA10, and GB30), and Mammoth (75CB1) subchrons.

6. A Positive Fold (Tilt) Test

[45] The mean paleomagnetic directions obtained for the stratoid series in the various tectonic blocks are summarized in Table 12. The declination and inclination differences with respect to the direction predicted for stable Africa at ~ 2 Ma are indicated. In order to check for the significance of these directions, we have attempted various «fold tests», which are listed in Table 13 [McElhinny, 1964; McFadden, 1990]. We have first calculated separate overall means for stratoid samples collected in Afar regardless of block or tectonic rotation. The overall means are statistically similar for reversed and normal samples and prior to and after tectonic correction. The values for the 231 combined normal and reversed sites (we use the same selection criteria on number of samples and confidence intervals for data gathered from previously published papers) are $D_g = 6.5^\circ$, $I_g = 15.3^\circ$ ($\alpha_{95} = 2.3^\circ$) and $D_s = 6.7^\circ$, $I_s = 13.5^\circ$ ($\alpha_{95} = 2.3^\circ$), respectively, before and after the correction, i.e., they are identical. The fact that many sites are actually flat lying and therefore entail no change upon «correction», and the fact that blocks with diverse tectonic rotations are

mixed would of course weaken any «fold test». The maximum dip of lava flows seldom exceeds 15° . We have attempted various selections (Table 13), and recalculated the means when only those sites with significant dip are included, or when only sites from nonrotated blocks are included. We have also recalculated these various means when all flows are considered separately or when assumed cooling units are used. The maximum changes entailed are on the order of 2° for I_g and 0.8° for I_s .

[46] The rock magnetic characteristics of the stratoid lavas, their young age, the brittle nature of the tectonics which affect them, the weak level of recent hydrothermal activity, dry climate and low alteration all argue in favor of a primary magnetization. Yet, in all of the attempts listed in Table 13, the 95% confidence intervals are almost unchanged upon tilt correction and there are no indications for a positive (or negative) fold test. It is of course disappointing that such a large collection of sites/flows from a single, locally tectonized, geological formation covering a wide geographical surface does not allow a fold test. We note that the Dobi block is unique among other nonrotated blocks within the Afar depression in that it is pervaded with significantly tilted (up to 20°) stretches of lava flows, all trending in the same WNW direction. We therefore compared the mean direction of flows from this block to the

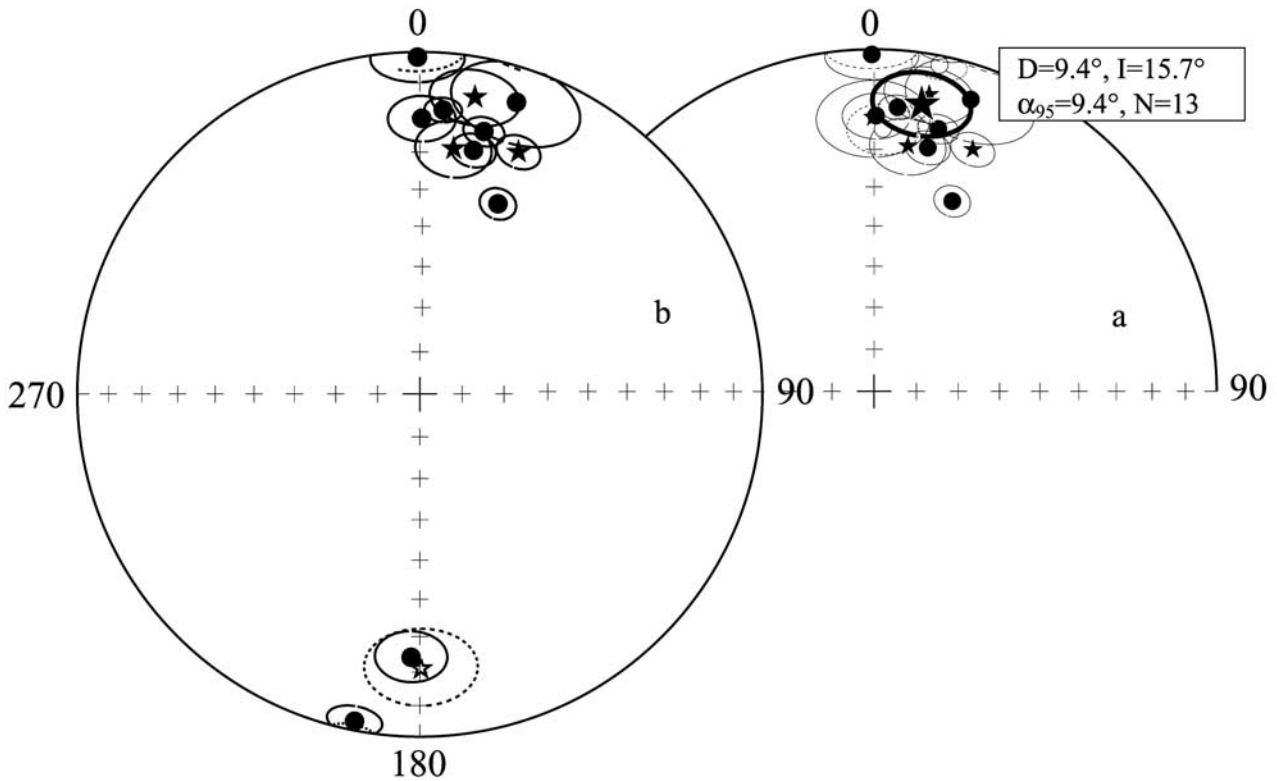


Figure 16. (a) Stereographic projections of characteristic magnetization directions (all flipped to normal polarity) from sites of stratoid series basalts in the two sections of the Isso-Deda'i block (see Figures 2 and 3c) and mean magnetization direction (large star with 95% confidence interval). Mean direction values are given in inset with statistical parameters (13 sites). (b) Individual site mean directions with original polarities. Small stars are from our section and circles from the *Acton et al.* [2000] section (see Table 8).

mean direction from all other nonrotated blocks (lower part of Table 13); all declinations are indeed close to 0. The inclination for blocks other than Dobi is hardly changed upon tilt correction, but for the Dobi block mean inclination goes from 22.5° to 10.1° (for flows, Table 13; from 25.9° to 13.5° for cooling units, Table 7) upon tilt correction. Application of the *McFadden and McElhinny* [1990] test to these directions yields a negative result prior to tilt correction (test parameter value $\gamma = 10.7^\circ$ versus a critical value $\gamma_c = 7.3^\circ$) and a positive one afterward ($\gamma = 4.3^\circ$, $\gamma_c = 7.0^\circ$). At the 95% confidence level, the directions are therefore compatible only in stratigraphic coordinates. This is the first time we have been able to demonstrate such a positive test, giving added strength to the conclusion that the characteristic magnetization in Afar stratoid lavas is indeed a primary one. We can therefore confidently analyze the implications, both geomagnetic and tectonic, of these directions, starting with inclinations.

7. Inclination Anomalies and Quadrupolar Fields

[47] The mean inclinations for each block, together with the differences between observed inclinations and those predicted by a geocentric axial dipole (GAD, from BC02) are listed in Table 12. We observe that 8 out of 10 values

are negative, but 8 are less than the 95% confidence interval and hence may not be statistically significant. The shallowing is almost significant in the Siyarrou block, and is certainly significant in the Gamarri section [*Kidane*

Table 8. Mean Paleomagnetic Directions for Two Nearby ~2 Ma Sections in the Isso-Deda'i Microblock (see Table 4)

Site	N	D_s	I_s	K	α_{95}
TDO14	6	179.8	-21.0	40.4	11.1
TDO16	6	10.5	12.7	64.2	8.4
TDO17	6	7.8	28.4	74.6	7.8
(TDO18)	6	21.1	25.4	75.8	7.7
(TDO19)	4	23.7	23.5	318.5	5.2
TDO18-19	10	22.2	24.6	114.5	4.5
ET022	6	191.3	3.0	194.5	4.8
ET023	4	181.9	24.2	164.0	7.2
(ET024)*	5	171.6	39.6	131.6	6.7
ET025	5	18.3	11.1	40.2	12.2
ET026-27	11	22.3	39.7	128.9	4.0
ET028	6	12.4	27.9	210.4	4.6
ET029	5	359.6	1.7	92.0	8.0
ET030	5	0.4	20.5	135.8	6.6
ET031-33	18	13.7	22.1	72.9	4.1
ET034	6	4.7	17.8	353.8	3.6
Mean: $D_s = 9.4^\circ$, $I_s = 15.7^\circ$ ($\alpha_{95} = 9.4^\circ$, $N = 13$, $K = 20.5$)					

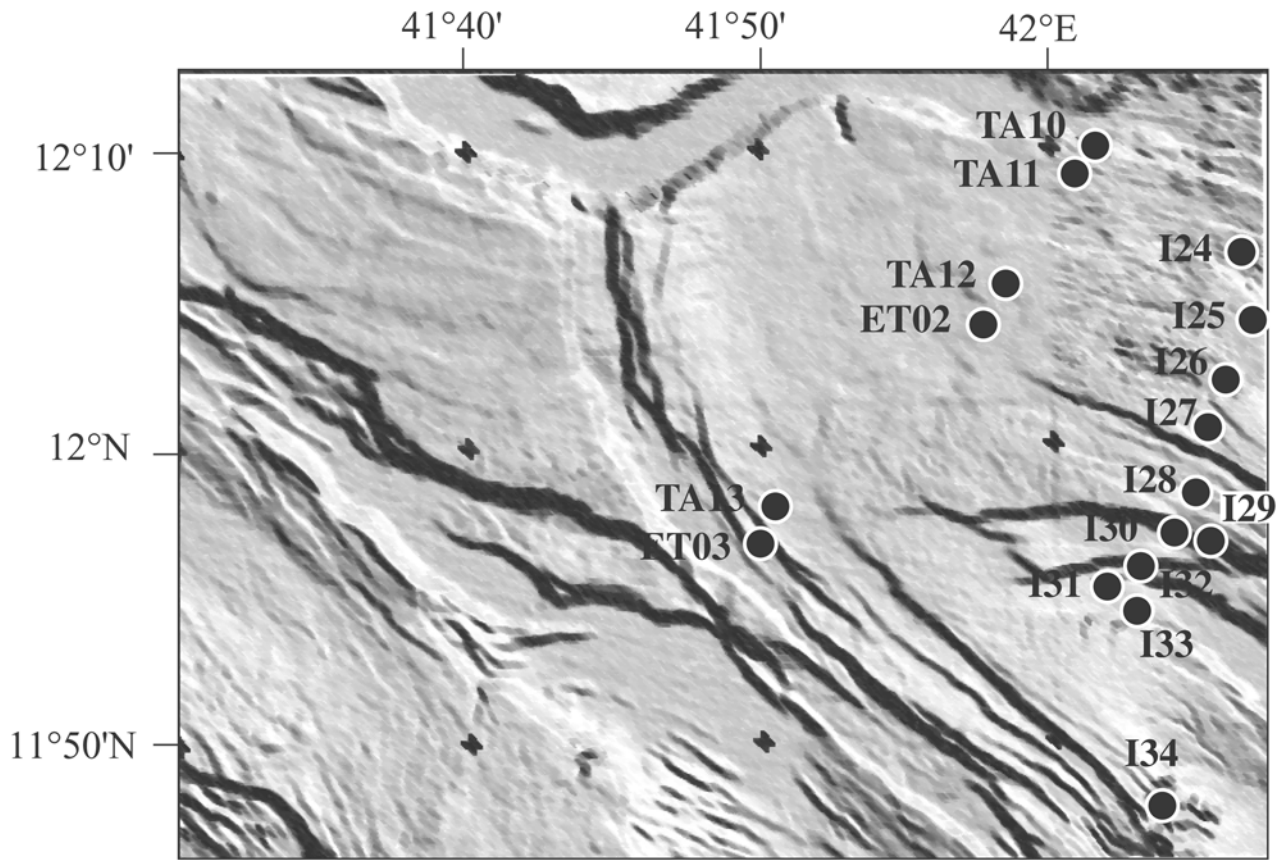


Figure 17. Detailed location of sites in Siyarrou block (see Figures 2 and 3c) with a rough indication of topography.

et al., 1999]. On the other hand, the anomaly is actually a significant steepening in the Der'Ela/Gaggade block.

[48] The fact that Afar lavas tend to have shallow inclination has been outlined in most previous studies [Courtillot *et al.*, 1984; Gruszow, 1992; Manighetti, 1993; Kidane *et al.*, 1999; Audin, 1999; Acton *et al.*, 2000]. When all 86 sites from nonrotated blocks are included (Table 13), the inclina-

tion anomaly (with respect to the 2 Ma GAD from BC02) is $-4.9 \pm 4.2^\circ$, and therefore appears to be significant. In order to enlarge the database to all sites, avoiding declination related effects, we have calculated an overall mean inclination anomaly based on «inclination only» data. Separate normal and reversed means are virtually identical and can therefore be combined. The overall mean for 229 flows

Table 9. Mean Paleomagnetic Directions for Sites in the Siyarrou Microblock (see Table 4)

Site	N	D _g	I _g	D _s	I _s	K _s	α _{95s}	Age (Ma)
TA10	6	346.8	19.0	346.8	19.0	66.8	9.2	0.94 ± 0.09 (recent bas.)
TA11	4	172.9	-9.6	172.9	-9.6	124.8	8.3	0.94 ± 0.04 (recent bas.)
TA12	5	178.2	-24.2	178.5	-9.1	66.0	9.8	0.85 ± 0.02 (recent bas.)
ET002	7	191.6	-10.6	191.6	-10.6	272.9	3.7	Recent basalts
Mean (Recent basalts): D _s = 357.5°, I _s = 12.2° (α ₉₅ = 12.9°, N = 4, K _s = 51.5)								
I24	8	186.4	-21.2	184.9	-26.1	314.0	3.2	Upper stratoid
I26	8	183.5	1.4	183.5	1.4	280.0	3.4	Upper stratoid
I30	8	179.2	13.7	179.2	13.7	174.0	4.3	Upper stratoid
I31	7	187.4	10.9	187.4	10.9	250.0	3.9	Upper stratoid
I33	4	201.9	-28.4	201.9	-28.4	236.4	7.0	Upper stratoid
I34	6	3.0	10.7	3.0	10.7	38.9	11.7	Upper stratoid
ET003-5	16	2.3	21.3	2.3	21.3	141.1	3.1	Upper stratoid
(TA13)	3	186.4	-24.5	183.6	-36.1	239.8	8.0	Upper stratoid (1.77 ± 0.06)
(I25)	6	185.4	7.0	185.4	7.0	183.0	5.1	Upper stratoid
(I27)	7	185.5	8.4	185.5	8.4	567.0	2.7	Upper stratoid
(I28)	7	186.0	5.0	186.0	5.0	408.0	3.1	Upper stratoid
(I29)	7	185.0	5.0	185.0	5.0	344.0	3.3	Upper stratoid
(I32)	7	183.8	7.5	183.8	7.5	280.0	3.7	Upper stratoid
I25,27-29,32	5	185.1	6.6	185.1	6.6	2181.1	1.6	Upper stratoid
Overall mean (Upper stratoid): D _s = 5.7°, I _s = 6.8° (α _{95s} = 12.8°, N = 8, K _s = 19.8)								

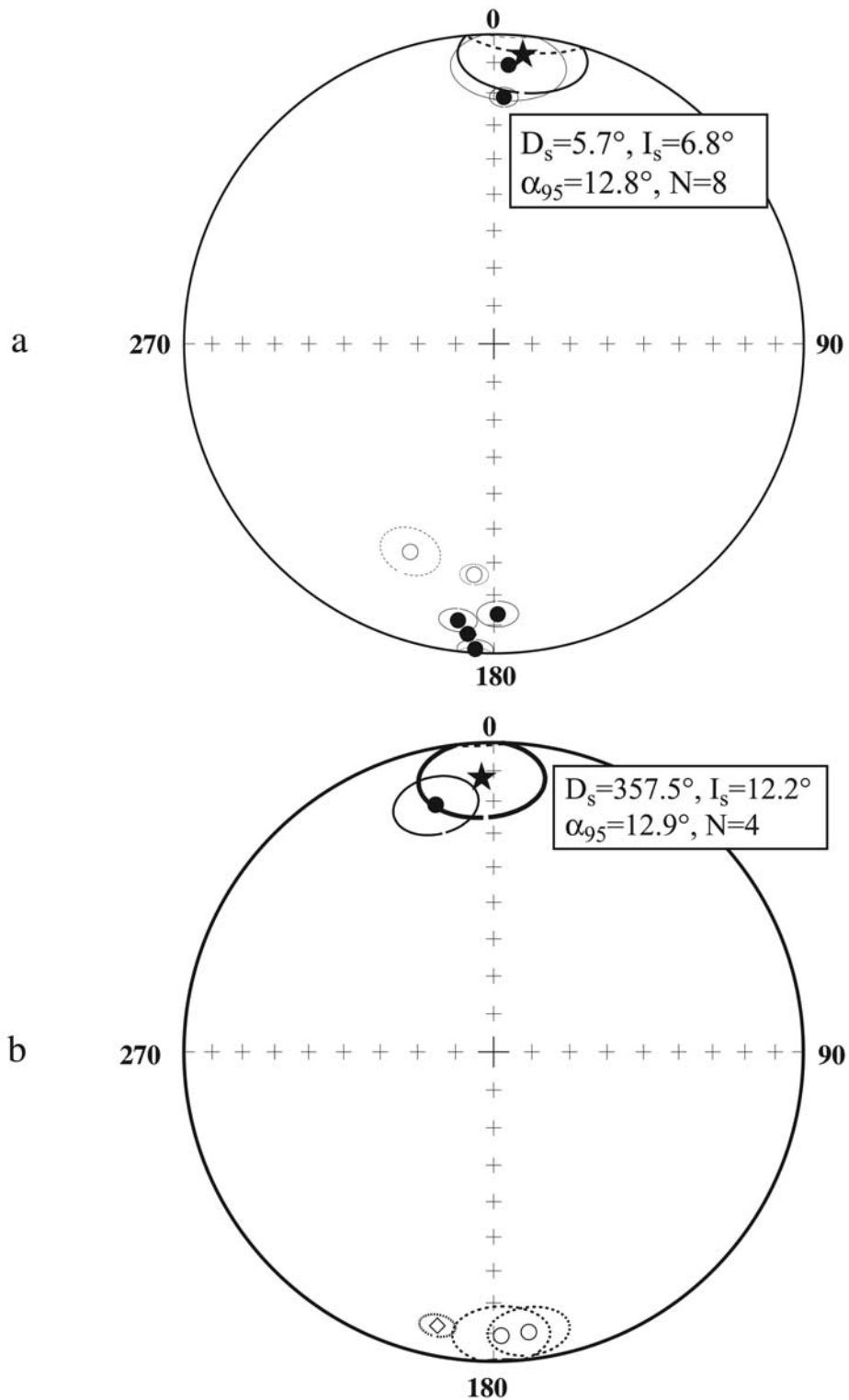


Figure 18. (a) Stereographic projections of characteristic magnetization directions from sites of stratoid series basalts in the Siyarrou block (see Figures 2 and 3c) and mean magnetization direction (stars with 95% confidence intervals). (b) Same for recent basalts. Mean direction values are given in insets with statistical parameters (4 and 8 sites, respectively) (see Table 9).

Table 10. Mean Paleomagnetic Directions for Sites in Recent Basalts North of the Immino Graben (see Table 4)

Site	N	D _g	I _g	D _s	I _s	K _s	α ₉₅
ET52	8	3.9	26.1	3.9	26.1	173.1	4.2
ET54-58	27	11.2	23.9	11.2	23.9	237.0	1.8
ET59	6	3.2	19.8	3.2	19.8	764.5	2.4
ET60	6	358.7	24.5	358.7	24.5	521.3	2.9
M13	6	5.3	27.8	3.2	28.1	364.9	3.9
M14	7	359.1	16.6	359.1	16.6	357.7	3.3
M15	8	6.3	31.0	4.9	34.4	722.1	2.1
M16	7	359.6	25.6	358.6	29.0	102.9	6.6
M19	7	355.7	18.9	355.7	18.9	196.0	4.4
M34	5	353.9	18.6	357.3	8.6	50.9	11.6
(M35-1)	4	32.5	21.3	31.9	26.1	36.4	16.4
(M35-2)	3	4.0	14.2	3.0	17.8	344.1	6.7
(M35-3)	3	342.8	33.6	339.7	35.6	999.9	2.4
M36	8	356.1	23.3	355.9	18.3	267.4	3.4
(I02-1)	4	343.8	29.2	343.8	29.2	154.2	8.6
(I02-2)	3	340.2	29.2	340.2	29.2	999.9	1.2
I02-1-2	7	341.9	29.2	341.9	29.2	326.7	3.4
I03-1	4	345.3	19.8	345.3	19.8	213.2	7.3
I03-2	4	344.0	25.7	344.0	25.7	684.2	3.7
(I04-1)	3	352.5	15.9	352.5	15.9	94.2	21.2
(I04-2)	3	354.7	13.7	354.7	13.7	533.3	8.8
I04-1-2	6	353.9	14.8	353.9	14.8	218.2	5.1
I16	6	351.5	25.9	351.5	25.9	136.9	6.4
C19	5	351.0	17.5	351.0	17.5	226.0	5.0
Mean: D _s = 356.4°, I _s = 22.6° (α ₉₅ = 4.3°, N = 17, K _s = 70.5)							

(Figure 21) is $-4.6 \pm 1.8^\circ$ (at the 95% confidence level), which is now strongly significant, and the median is -3.7° . The standard deviation is 14.3° , i.e., a typical record of secular variation. As seen in Figure 21, the inclination anomaly distribution is slightly skewed, with more observations in the $+5^\circ/-5^\circ$ range, and less in the $-10^\circ/-30^\circ$ range, except for a secondary maximum at -25° . Some of these values may come from oversampling in the helicopter traverse of the Siyarrou and north Immino blocks by *Man-*

ighetti [1993]. When these six values are removed, the mean becomes $-4.0 \pm 1.8^\circ$, and the median -3.1° .

[49] The above discussion leads us to believe that sampling difficulties, tectonic problems, laboratory problems, remagnetization, secular variation, or age distribution cannot be responsible for these shallow inclinations. The shallow inclinations are in the sense observed by *Wilson* [1971] and compatible with his interpretation of a standing axial quadrupolar component in the long-term mean geomagnetic field. Recent analyses [*Quidelleur et al.*, 1994; *Johnson and Constable*, 1995, 1997; *Carlut and Courtillot*, 1998] all lead to mean quadrupolar terms g_2° on the order of 3–6% of the main axial dipole g_1° . The inclination anomaly observed in the Afar stratoid series would lead, if taken alone and at face value, to a quadrupolar term of $6 \pm 2\%$ at the 95% confidence level. The Fisherian average would lead to a value of $6 \pm 5\%$. Following the analysis by *Carlut et al.* [2000] of sensitivity of global field model coefficients to a single datum, we find that inclusion of our inclination value hardly changes the value of g_2° in a mean field model for the last 5 Ma (a few per mil, clearly not significant). Larger changes, on the order of 20% and 40% occur in degree 3 and 4 terms, respectively. These changes do not stand out significantly above the noise level [*Carlut et al.*, 2000]. This result is not surprising since data from Europe, North Africa, and western Africa already constrained the model strongly on a regional scale. Moreover, most regional data, which date from the 1970s, indeed indicated negative inclination anomalies [*Johnson and Constable*, 1995; *Carlut*, 1998; *Carlut and Courtillot*, 1998], despite small numbers of lava flows and often moderate experimental quality. Such was the case for Guinea (-8°), Ghana (-7°), Lybia (-13°), and Lebanon (-5°). This led in previous degree 4 mean field models to a regional inclination anomaly of about -3° [*Carlut*, 1998, p. 334]. Accounting for the slightly larger Afar inclination anomaly which we

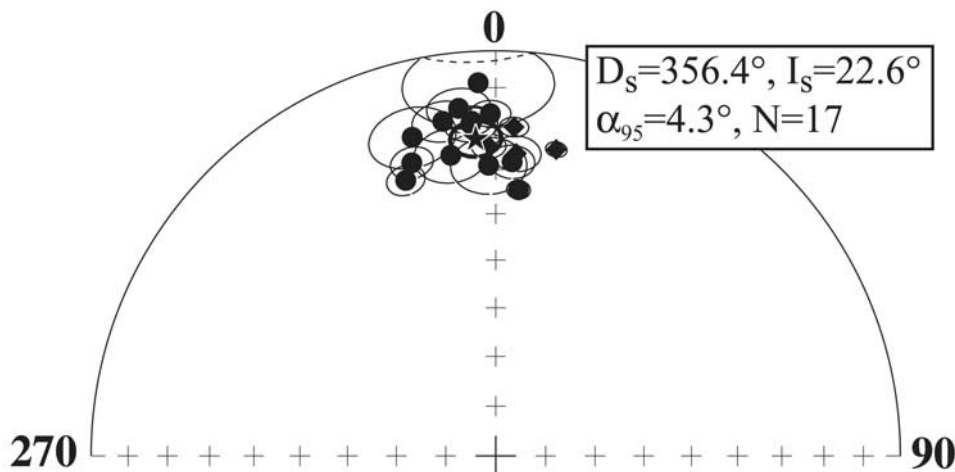


Figure 19. Stereographic projections of characteristic magnetization directions from all sites of stratoid series basalts available from previous publications north of Immino graben (see Figures 2 and 3c) and mean magnetization direction (star with 95% confidence intervals). Mean direction value is given in inset with statistical parameters (17 sites) (see text and Table 10 for references to previous publications).

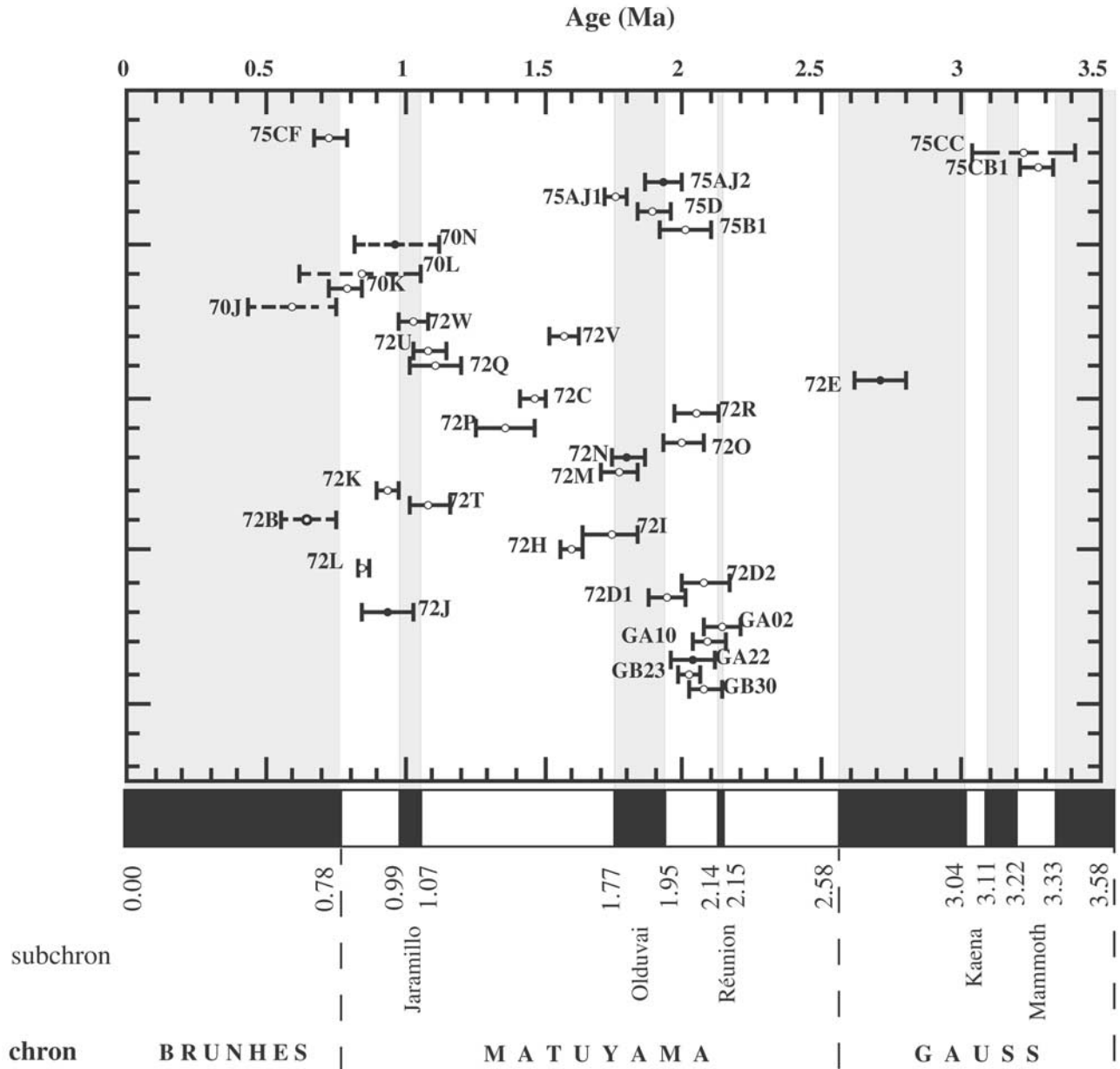


Figure 20. Summary of all ages obtained in this paper with 1σ uncertainties compared to the geomagnetic polarity timescale of *Cande and Kent* [1995]. Chrons and subchrons are indicated and likewise sample magnetic polarity (open circle = reversed, full circle = normal, thick circle = intermediate). Five samples with larger uncertainties are shown as dashed segments (see text).

obtain here ($-4^{\circ}/-5^{\circ}$) does not require a larger global quadrupole.

8. Declination Anomalies, Rotations, and Rift Propagation

[50] The declination differences listed in Table 12 can be interpreted in terms of block rotations about vertical axes. We note that the mean direction obtained from the 26 sites scattered over the Ethiopian (Mile-Gewane) and Somalian (Ali Sabieh) parts of the studied area to the south of the main escarpment that limits the Afar depression is virtually

identical to the expected one. This mean overall direction is representative of the “stable” part of the African plate. The corresponding VGP for the period 1–3 Ma is located at $\lambda = 87.2^{\circ}\text{N}$, $\phi = 217.1^{\circ}\text{E}$ ($A_{95} = 4.0^{\circ}$). This direction can be used as a new reference in place of the BC02 synthetic prediction ($\lambda = 86.7^{\circ}\text{N}$, $\phi = 174.9^{\circ}\text{E}$; $A_{95} = 2.9^{\circ}$) to calculate the rotations between individual blocks and stable Africa. These are given in the last column of Table 12. The new data from Ethiopian Afar given in this paper, combined with those of *Acton et al.* [2000], can be added to already available ones from Djiboutian Afar [mainly *Courtilot et al.*, 1984; *Manighetti*, 1993; *Audin*, 1999; *Manighetti et al.*,

Table 11. Correlation of Ages and Magnetic Polarities Obtained in This Paper With the Geomagnetic Polarity Timescale (GPTS) From *Cande and Kent* [1995]

Paleomagnetic Site (Code Name)	Geochronologic Site (Code Name)	Age, Ma (This Paper)	Polarity (and Subchron) (This Paper) ^a	Age of Polarity Chron in GPTS, Ma
TA01	72B	0.65 ± 0.10	T-within Brunhes?	0.00–0.78?
TA31	75CF	0.73 ± 0.06	N-Brunhes	0.00–0.78
TA10	72J	0.94 ± 0.09	N-Jaramillo	0.99–1.07
TA14	72N	1.80 ± 0.06	N-Olduvai	1.77–1.95
TA13	72M	1.77 ± 0.06	R-Matuyama	0.780–2.58
TA03	72D1	1.94 ± 0.07	R-Matuyama	0.780–2.58
TA04	72D2	2.08 ± 0.08	R-Matuyama	0.780–2.58
TA12	72L	0.85 ± 0.02	R-Matuyama	0.780–2.58
TA08	72H	1.60 ± 0.04	R-Matuyama	0.780–2.58
TA21	72T	1.09 ± 0.07	R-Matuyama	0.780–2.58
TA15	72O	2.00 ± 0.07	R-Matuyama	0.780–2.58
TA17	72P	1.36 ± 0.11	R-Matuyama	0.780–2.58
TA20	72R	2.05 ± 0.08	R-Matuyama	0.780–2.58
TA06	72C	1.46 ± 0.05	R-Matuyama	0.780–2.58
TA18	72Q	1.11 ± 0.09	R-Matuyama	0.780–2.58
TA22	72U	1.09 ± 0.06	R-Matuyama	0.780–2.58
TA23	72V	1.57 ± 0.05	R-Matuyama	0.780–2.58
TA24	72W	1.03 ± 0.05	R-Matuyama	0.780–2.58
TDO01	75B1	2.01 ± 0.09	R-Matuyama pre-Olduvai	0.780–2.58
TDO07	75D	1.89 ± 0.06	R-Matuyama pre-Olduvai	0.780–2.58
TDO14	75AJ1	1.76 ± 0.04	R-Matuyama post-Olduvai	0.780–2.58
TDO19	75AJ2	1.93 ± 0.07	N-Olduvai	1.77–1.95
TA05	72E	2.71 ± 0.09	N-Gauss	2.58–3.58
TA25	75CB1	3.27 ± 0.06	R-Mammoth	3.22–3.33
TA40	75CC	3.22 ± 0.05	R-Mammoth	3.22–3.33
TA11	72K	0.94 ± 0.04	R-Matuyama	0.780–2.58
TA09	72I	1.74 ± 0.10	R-Matuyama	0.780–2.58
LO01	70J	0.59 ± 0.16	R-Matuyama pre-Brunhes?	0.780–2.58?
LO02	70K	0.79 ± 0.06	R-Matuyama	0.780–2.58
LO06C1	70L	0.84 ± 0.22	R-Matuyama	0.780–2.58
LO08	70N	0.97 ± 0.15	N-Jaramillo	0.99–1.07

^aN, normal polarity; R, reversed; and T, transitional.

2001a]. The mean directions and rotations for blocks located in Djiboutian Afar are listed in Table 12. Replacement of the BC02 reference direction by that obtained in this paper barely changes the rotation angles (by 2.7°) and increases the 95% uncertainties by 1 to 2°. However, it does not change whether rotation estimates are significantly different from zero or not. These rotations are displayed for each block in Figure 2. As already known, the three (first-order) eastern blocks of Der’Ela-Gaggade, Data-Yager-Hanle, and Gamarri-Dakka have suffered significant

clockwise rotations between 12 and 18°, with 95% uncertainties between 7 and 9°. These rotations are not significantly different from each other.

[51] In contrast, the three western first-order blocks, which form the NW extension of the eastern ones, i.e., Siyarrou/Isso-Deda’i, Dobi, and Unda-Gamarri, have not suffered significant rotations: (angles between 0 and 9°; 95% uncertainties between 7 and 14°). This is consistent with the tectonic interpretation of the NE trending Gamarri-Alol tear zone, which marks the locus where the NW-

Table 12. Mean Paleomagnetic Directions Obtained in the Present Study for the Stratoid Formation in Central Afar

Block	N	D _s (°) (δD)	I _s (°) (δI)	Rotation 1 (ΔD)	Shallowing (ΔI)	Rotation 2 (ΔD)
Results from this paper (Ethiopian or Central Afar) ^a						
Mile-Gewane Ali Sabieh	26	359.7° (5.9°)	16.4° (5.7°)	-2.7 ± 6.6°	-0.7 ± 6.3°	0 ± 5.9°
Unda-Gamarri	17	0.0° (7.5°)	17.9° (7.2°)	-2.4 ± 8.0°	-0.1 ± 7.7°	0.3 ± 9.5°
Dobi	20	1.1° (7.6°)	13.5° (7.4°)	-1.3 ± 7.8°	-4.5 ± 7.9°	1.4 ± 9.6°
Isso-Deda’i	13	9.4° (9.7°)	15.7° (9.4°)	6.9 ± 10.1°	-3.3 ± 9.8°	9.7 ± 11.3°
Siyarrou	8	5.7° (12.9°)	6.8° (12.8°)	3.2 ± 13.2°	-12.2 ± 13.1°	6.0 ± 14.2°
Gamarri Section	27	8.1° (4.0°)	10.1° (4.1°)	5.7 ± 4.9°	-7.9 ± 5.0°	8.4 ± 7.1°
Results from earlier studies (Djiboutian or East Afar) ^b						
Gamarri-Dakka	12	12.4° (7.8°)	16.2° (8.1°)	10.0 ± 8.3°	-1.8 ± 8.6°	12.7 ± 9.8°
Data Yager-Hanle	23	15.8° (5.1°)	16.7° (5.3°)	13.4 ± 5.9°	-1.3 ± 6.0°	16.1 ± 7.8°
Der’Ela-Gaggade	13	17.8° (6.2°)	28.1° (7.1°)	15.4 ± 6.8°	10.1 ± 7.6°	18.1 ± 8.6°
Region North of Balho	11	0.5° (10.8°)	19.8° (11.5°)	-2.0 ± 11.2°	0.8 ± 11.8°	0.8 ± 12.3°

^aFor the different blocks discussed in the text, see Figure 2a. Rotation 1 (ΔD) and Shallowing (ΔI) are calculated as the differences between the mean observed declination and inclination and those predicted at ~2 Ma by *Besse and Courtillot* [2002], i.e., D = 2.4° (δD = 2.9°), I = 18.0° (δI = 2.8°) at 11°30’N, 41°30’E; rotation 2 is referred to the Mile-Gewane/Ali Sabieh average taken as a new reference for stable Africa (see text).

^bSame for earlier results from eastern Afar [*Manighetti*, 1993; *Courtillot et al.*, 1984]. See also Table 1.

Table 13. Mean Paleomagnetic Directions of Sites/Flows of the Stratoid Series for Different Groupings (N is for Normal Sites, \bar{R} for Flipped Reversed Sites)^a

	N	D _g	I _g	(α_{95}) _g	K _g	D _s	I _s	(α_{95}) _s	K _s	K _s /K _g
<i>All Sites</i>										
N	74	9.5	16.6	4.1	17.4	9.4	14.5	4.1	17.2	0.99
\bar{R}	157	5.0	14.6	2.7	18.4	5.4	13.0	2.7	18.4	1.00
N + \bar{R}	231	6.5	15.3	2.3	17.9	6.7	13.5	2.3	17.9	1.00
<i>All Sites With Significant Dip</i>										
N	37	8.3	19.1	5.4	20.2	8.2	16.0	5.4	20.2	1.00
\bar{R}	74	3.8	15.4	3.9	18.6	4.7	12.1	3.9	18.9	1.02
N + \bar{R}	111	5.3	16.6	3.2	18.9	5.9	13.4	3.1	19.2	1.02
<i>All Sites From Nonrotated Blocks</i>										
N	25	1.2	20.7	5.7	27.0	2.2	13.6	5.5	29.0	1.07
\bar{R}	61	358.8	15.2	4.0	21.5	0.0	12.8	4.0	23.1	1.07
N + \bar{R}	86	359.5	16.8	3.3	22.6	0.6	13.1	3.1	24.7	1.09
<i>All Sites From Nonrotated Blocks Except Dobi</i>										
N	12	358.5	18.6	10.5	18.1	0.6	17.5	9.6	21.4	1.18
\bar{R}	51	359.5	13.7	4.4	21.3	0.1	13.4	4.3	22.2	1.04
N + \bar{R}	63	359.3	14.6	4.0	20.7	0.2	14.2	3.9	22.2	1.07
<i>All Sites From Dobi Block Only</i>										
N	13	3.6	22.5	6.0	48.7	3.6	10.1	6.1	47.5	0.98
\bar{R}	10	355.3	22.3	9.4	27.7	359.3	10.2	9.4	27.7	1.00
N + \bar{R}	23	0.0	22.5	5.2	35.4	1.8	10.1	5.0	37.1	1.05

^an is number of sites/flows, D, I, α_{95} , and K are declination, inclination, 95% confidence interval, and Fisher's precision parameter, with subscript g for geographic/in situ and s for stratigraphic/tectonically corrected values.

striking fault-bounded blocks suffer right-stepping and break along numerous, small, more easterly striking normal faults [Manighetti *et al.*, 2001a].

[52] The stratoid formation, which floods the floor of the Afar, forms a vast morphologic reference surface whose topography has recorded all tectonic deformations which affected it in the last 2–3 million years. Our new data are in agreement with the “two phase” model of rift propagation, overlap and bookshelf faulting recalled in the introduction. After a period (~20–5 Ma) when motion in the Gulf of Aden was transferred to southern Afar through the Shukra-el-Sheik transform fault and its onland extension as the Bia Anot fault (Figures 1 and 3a), the Gulf of Aden rift propagated westward between 5 and 2 Ma to the entrance of the present-day gulf of Tadjoura. There, it established a new transform system to the south, extending onland as the Hol Hol fault system (Figures 1 and 3a) and branching in horse tail fashion to the west and then WNW. In the same period, the Red Sea rift had extended to the south, creating (an ancestor of) the Manda-Hararo rift. This intersected the preexisting and only weakly active northern termination of the East African rift, and that part of Africa to the south of the large escarpment was left relatively unaffected.

[53] Such was the situation about 4–3 Ma ago, when the stratoid series began to be emplaced through a broad set of NW-SE trending fissures and covered most of the previous (Dahla) volcanic products, which now outcrop only at the edges of the Afar depression. Whereas the Manda-Hararo rift remained active in the same general configuration, the gulf of Aden once again propagated westward between 2 and 1 Ma, creating the Asal-Ghoubbet rift about 0.9 Ma ago. There was therefore an overlap between the Asal-

Ghoubbet and Manda-Hararo rifts, bounded to the west by what is approximately now the Gamarri-Alol zone and to the east by the Hol Hol fault zone. This initial overlap zone functioned between about 0.9 and 0.2 Ma, with its fault-bounded elongate blocks rotating following a bookshelf mechanism [Tapponnier *et al.*, 1990; Manighetti *et al.*, 2001a]. About 200,000 years ago, the Gulf of Aden rift once again propagated as a right step to the NW, generating the Mak'arrasou transfer zone, and the Manda-Inakir rift. This more than doubled the size of the overlap between the two main rift branches and initiated faulting and bookshelf rotation of the north Immimo, Siyarrou, Isso-Dobi, and Unda-Gamarri blocks. The propagation and plate kinematics allow rotation amplitudes to be predicted [Manighetti, 1993; Manighetti *et al.*, 2001a], leading to estimates of $13 \pm 1.5^\circ$ for all blocks belonging to the first, older overlap SE of Gamarri-Alol, and only $2 \pm 0.2^\circ$ for the blocks in the younger overlap to the NW of it. These are all in agreement with observations (Table 12 and Figure 2).

[54] The southernmost part of the Dobi graben, within the Gamarri-Alol transfer zone, could have been expected to have rotated by an amount similar to the Data-Yager block, i.e., by some 10° . Yet, the declination anomaly is almost zero (Table 12), contrary to neighboring blocks. Based on seismic and structural evidence, Jacques [1995] proposed that this small area may have suffered a second, smaller-scale phase of bookshelf faulting, linked directly to right-stepping between the Hanle and Dobi grabens. Indeed, the small and elongated basaltic strips, oriented $N110^\circ E \pm 10^\circ$, are involved in an overall sinistral shear, which must have led to anticlockwise rotation. The small region could therefore have suffered a succession of a $\sim 10^\circ$ clockwise rotation linked to the large, older Asal-Ghoubbet/Manda-Hararo-Abhe overlap, canceled by a $\sim 10^\circ$ but counterclockwise rotation due to sinistral shear linked with the right-stepping basins. This would imply that the SE Dobi faults originally trended $N120^\circ E$, which is actually perpendicular to the regional extensional direction. The analysis of Jacques [1995] is therefore in agreement with the paleomagnetic direction we observe.

[55] The Siyarrou and Isso sites indicate clockwise rotations ($6 \pm 14^\circ$ and $10 \pm 13^\circ$, respectively) which are not significantly different from zero but are intermediate between the larger rotations to the SE and the smaller, negligible ones to the north and west. The SE terminations of these blocks might have been entrained or have belonged to the NW termination of the first generation rotating overlap.

[56] Overall, the propagation model predicts sizable rotations only in areas where a significant overlap occurred and was maintained long enough. The first-order blocks and two subsequent geometries of the overlap zone between the Gulf of Aden and Red Sea rift terminations are consistent with the paleomagnetic results, and so is at second-order level, the geometry and structural significance of the Gamarri-Alol tear zone.

[57] Our data extend the coverage of Ethiopian Afar published by Acton *et al.* [2000]: their data, together with our new age determinations, are included in the above analysis. Based on their own, and our earlier data, Acton *et al.* [2000] produced a tectonic analysis which we now

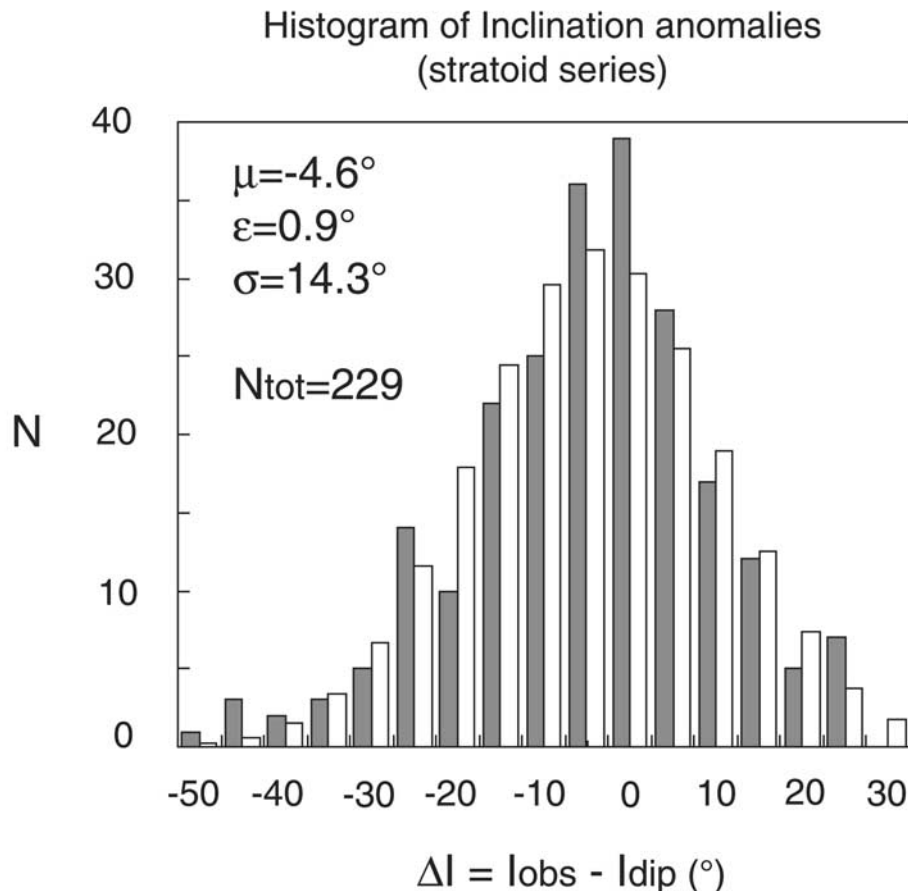


Figure 21. Distributions of inclination anomalies (gray bars) for all flows/sites of stratoid basalts measured or compiled in this study (except 2 transitional directions). Inclination anomaly is difference between measured inclination of site characteristic direction and expected value at same location and relevant age from the study of *Besse and Courtillot* [2002] synthetic APWP for Africa. The best-fit Gaussian distribution is shown as white bars, and the corresponding mean μ , uncertainty on the mean ε , and standard deviation σ (all in degrees) and total number of sites are given.

discuss. *Acton et al.* [2000] refer rotations to the expected geocentric axial dipole direction in Afar. This results in ~ 3 to 4° clockwise rotations for the blocks of central Afar (i.e., NW of the Gamari-Alol tear zone) and ~ 7 to 11° for blocks in eastern Afar (i.e., Djiboutian Afar). *Acton et al.* calculate an overall average for all of central Afar ($3.6 \pm 4.4^{\circ}$) which is not significantly different from zero. The value we obtain for all our “nonrotated” sites is $2.0 \pm 4.5^{\circ}$, and leads to the same conclusion. *Acton et al.* propose two alternate scenarios. The first, preferred one, has a lot in common with ours, based on the idea that block rotations are linked and evolve together with rift propagation [see *Courtillot et al.*, 1984]. However, there are some important, though possibly second-order differences, based on actual field and tectonic observations. For instance they have the rotations beginning at 1.8 Ma, when *Manighetti et al.* [2001a] show that it should be 0.9 Ma when overlap began; their model implies rifting in the Bada Wein flats which is not observed; they introduce two large NE-SW trending faults to account for variations in rotations, when these two faults are not found in the field;

finally, they invoke large opening in the central Afar fault systems, which they call rifts, where we find a maximum of some 15% horizontal strain. *Acton et al.*'s [2000] second scenario assumes that the Asal-Manda-Inakir active zone is already the established plate boundary between Arabia and Africa, which would imply that the Manda-Hararo zone should be inactive. Actually, both the southern termination of the Red Sea propagator (Arabia versus Nubia) and the western termination of the Aden propagator (Arabia versus Somalia) are active. This scenario would also imply that propagation velocity of the Aden rift has increased from east (Asal and east of it) to west (central Afar and Manda-Inakir), whereas this velocity has been found rather constant at 10–20 cm/yr at all scales [*Manighetti et al.*, 2001a]. Altogether, the main differences between *Acton et al.*'s [2000] model and ours, which belong to the same family of plate kinematic models, are due to the duration over which the blocks are assumed to retain rigidity and a clear identity (a few Ma versus a few hundred ka), and in our case to the inclusion of numerous field data.

9. Conclusion

[58] The model of rift propagation and overlap in the Afar depression is based on observations concentrated in the Republic of Djibouti and at sea, and makes prediction in the larger, previously little explored, Ethiopian part of central Afar. In this paper, we have reported a series of 24 new K-Ar age determinations and 98 new paleomagnetic site (flow) mean directions, covering the northernmost part of stable Africa, to the south of the Afar depression and on both sides of the termination of the East African rift, and five blocks within central Afar, previously identified by structural analysis. These new data, combined with previous ones, allow to test models of rift propagation and deformation in the area.

[59] The ages of sampled lava flows range from 3.3 to 0.6 Ma, with data being concentrated around ~ 2 Ma. Three different subunits are recognized within what was previously mapped as the single stratoid series: we refer to them as lower stratoid, upper stratoid and recent (or “Gulf”) basalts. We mainly focus our discussion on data from the upper stratoid formation at ~ 2 Ma. Extensive amounts of new K-Ar data covering a wider area and a larger age range are published by *Lahitte et al.* [2001]. Based on this larger data set, the age distribution (between 3 and 0.5 Ma) is found to be more continuous than previously suggested, with evidence that the earliest stratoid activity propagated from south to north at approximately 10 cm/yr within the depression. This is consistent with the data and interpretations of Audin et al. (submitted manuscript, 2002), who show that propagation of the Gulf of Aden into Afar implied a first phase of deformation along the Shukra-el-Sheik (at sea) and Bia Anot (on land) transform faults, connecting to the ancestor of the Manda-Hararo rift system (Figure 1).

[60] We now have a database of 231 paleomagnetic mean flow directions for the stratoid series alone. Magnetization is bimodal and mostly carried by titanium-poor magnetites, and a ChRM is rather easily extracted from most samples; AF treatment is generally the most efficient to determine this ChRM. Among several tilt tests performed on subsets of this large database, one provided a clearly positive result, when directions from all nonrotated, dominantly flat-lying flows were compared to those in the tectonically active and tilted Dobi block. This and other lines of evidence point to the primary nature of magnetization. Analysis of the magnetic polarity of dated samples yields 36 new results, most of which are in agreement with the GPTS of *Cande and Kent* [1995]. Eight samples have age uncertainties less than 50 kyr and can be used as constraints in future reassessments of transition times, particularly the upper Olduvai/Matuyama and lower Olduvai/Matuyama reversals, and the Reunion and Mammoth subchrons.

[61] Comparison of observed directions with those predicted by *Besse and Courtillot* [2002] for stable Africa confirms that Afar inclinations are generally on the low side. An analysis of inclinations from 231 flows of the ~ 2 Ma stratoid series yields a significant shallowing of $-4.6 \pm 1.8^\circ$, consistent with generally accepted values for a global axial quadrupole ($g_2/g_1^\circ = 6 \pm 2\%$). Inclusion of this new datum in the 0–5 Ma database and subsequent inversion does not change mean field coefficients in a significant manner.

[62] Results from the Mile-Gewane and Ali Sabieh blocks yield a new reference pole for stable Africa at 2.0 (± 1) Ma. The pole lies at $\lambda = 87.2^\circ\text{N}$, $\phi = 217.1^\circ\text{E}$ ($N = 26$ sites, $A_{95} = 4.0^\circ$). Rotations of blocks located to the east and north of the Gamarri Alol tear zone are (rounded to the nearest degree and computed with respect to the local, Mile-Gewane/Ali Sabieh, estimate of a stable African reference direction) $0 \pm 9^\circ$, $1 \pm 10^\circ$, $10 \pm 11^\circ$, $6 \pm 14^\circ$, and $1 \pm 12^\circ$, respectively, for the Unda-Gamarri, Dobi, Isso-Deda’i, Siyarrou, and north Balho microblocks. This compares with $13 \pm 10^\circ$, $16 \pm 8^\circ$, $18 \pm 9^\circ$, and $8 \pm 7^\circ$, respectively, for the Gamarri-Dakka, Data-Yager-Hanle, and Der’Ela-Gaggade blocks and the Gamarri cliff section. Taken altogether, the declination difference for the nonrotated blocks is 2° ($\pm 4^\circ$), whereas it is 13° ($\pm 4^\circ$) in the rotated ones. These values are in excellent agreement with those predicted by the rift propagation/overlap model of *Manighetti et al.* [2001a], which are 2° ($\pm 0.2^\circ$) and 13° ($\pm 1.5^\circ$), respectively.

[63] The bookshelf faulting model is consistent with the bulk of new data reported in this paper. The spatial amplitude of overlap and duration when a given overlap configuration holds are the parameters which control the total rotation of any single block, given the boundary conditions of plate velocity. Therefore, the same physical process seems to have been at play in central Afar for the last 4 Myr.

[64] **Acknowledgments.** The paleomagnetic software package PaleoMac, used throughout this work, was developed and has been continuously upgraded and expanded by J.P. Cogné, whom we gratefully acknowledge. We also acknowledge the friendly support of Salomon Tadesse and Gezahegn Yirgu in managing the joint Ethiopian-French geodynamics project and of many colleagues in Addis Ababa and in the field in central Afar for their help. We thank Gary Acton for discussions, for making his entire data readily accessible to us, and for a helpful review. This is IPGP contribution 1873.

References

- Acton, G. D., S. Stein, and J. F. Engeln, Block rotation and continental extension in Afar: A microplate model for Afar, *Tectonics*, 10, 501–526, 1991.
- Acton, G. D., A. Tessema, M. Jackson, and R. Bilham, The tectonic and geomagnetic significance of paleomagnetic observations from volcanic rocks from central Afar, Africa, *Earth Planet. Sci. Lett.*, 180, 225–241, 2000.
- Audin, L., Pénétration de la dorsale d’Aden dans la dépression Afar entre 20 et 4Ma, Ph.D. thesis, 318 p., Univ. de Paris VII and Inst. de Phys. du Globe de Paris, Paris, 1999.
- Baker, B. H., P. Mohr, and L. A. J. Williams, Geology of the eastern rift system of Africa, *Geol. Soc. Am. Spec. Pap.*, 136, 1–67, 1972.
- Barberi, F., H. Tazieff, and J. Varet, Volcanism in the Afar depression: Its tectonic and magmatic significance, *Tectonophysics*, 15, 19–29, 1972.
- Barberi, F., R. Ferrara, R. Santacroce, and J. Varet, *Structural Evolution of the Afar Triple Junction*, edited by A. Pilger and A. Rösler, pp. 39–53, Schweizerbart, Stuttgart, 1975.
- Besse, J., and V. Courtillot, Revised and synthetic apparent polar wander paths of the African, Eurasian, North American and Indian plates, and true polar wander since 200 Ma, *J. Geophys. Res.*, 96, 4029–4050, 1991.
- Besse, J., and V. Courtillot, Apparent and true polar wander and the geometry of the geomagnetic field in the last 200 million years, *J. Geophys. Res.*, 107(B11), 2300, doi:10.1029/2000JB000050, 2002.
- Black, R., W. H. Morton, and D. C. Rex, Block tilting and volcanism within the Afar in light of recent K/Ar data, in *Afar Depression of Ethiopia*, edited by A. Pilger and A. Rösler, pp. 296–299, Schweizerbart, Stuttgart, 1975.
- Cande, S. C., and D. V. Kent, Revised calibration of the geomagnetic polarity timescale for the Late Cretaceous and Cenozoic, *J. Geophys. Res.*, 100, 6093–6095, 1995.
- Carlut, J., Caractéristiques spatiales et temporelles du champ magnétique terrestre à l’échelle des temps géologiques (10^4 – 10^6 ans), Ph.D. thesis, 348 pp., Univ. Paris VII and Inst. de Phys. du Globe de Paris, Paris, 1998.

- Carlut, J., and V. Courtillot, How complex is the time-averaged geomagnetic field over the past 5 million years?, *Geophys. J. Int.*, 134, 527–544, 1998.
- Carlut, J., X. Quidelleur, V. Courtillot, and G. Boudon, Paleomagnetic directions and K/Ar dating of 0 to 1 Ma old lava flows from La Guadeloupe Island (French West Indies): Implications for time averaged field models, *J. Geophys. Res.*, 105, 835–849, 2000.
- Cassignol, C., and P. Y. Gillot, Range and effectiveness of unspiked potassium–argon dating in *Numerical Dating in Stratigraphy*, edited by G. S. Odin, pp. 159–172, John Wiley, New York, 1982.
- Champion, D. E., M. A. Lanphere, and M. A. Kuntz, Evidence for a new geomagnetic reversal from lava flows in Idaho: Discussion of short polarity reversals in the Brunhes and late Matuyama polarity chrons, *J. Geophys. Res.*, 93, 11,667–11,680, 1998.
- Chessex, R., M. Delaloye, J. Muller, and M. Weidmann, Evolution of the volcanic region of Ali Sabieh (TFAI), in light of K/Ar age determinations, in *Afar Depression of Ethiopia*, edited by A. Pilger and A. Rösler, pp. 221–227, Schweizerbart, Stuttgart, 1975.
- Civetta, L., M. De Fino, P. Gasparini, M. R. Ghiara, L. La Volpe, and L. Lirer, Structural meaning of east-central Afar volcanism (Ethiopia, T.F.A.I.), *J. Geol.*, 83, 363–373, 1975.
- Courtillot, V., Opening of the Gulf of Aden and Afar by progressive tearing, *Phys. Earth Planet. Inter.*, 21, 343–350, 1980.
- Courtillot, V., Propagating rifts and continental breakup, *Tectonics*, 1, 239–250, 1982.
- Courtillot, V., A. Galdéano, and J. L. Le Mouél, Propagation of an accreting plate boundary: A discussion of new aeromagnetic data in the Gulf of Tadjurah and Southern Afar, *Earth Planet. Sci. Lett.*, 47, 144–160, 1980.
- Courtillot, V., J. Achache, F. Landre, N. Bonhommet, R. Montigny, and G. Féraud, Episodic spreading and Rift propagation: New paleomagnetic and geochronological data from the Afar nascent passive margin, *J. Geophys. Res.*, 89, 3315–3333, 1984.
- Courtillot, V., R. Armijo, and P. Tapponnier, Kinematics of the Sinai triple junction and a two-phase model of Arabia–Africa rifting, in *Continental Extensional Tectonics*, edited by M. P. Coward, J. F. Dewey, and P. L. Hancock, *Spec. Publ. Geol. Soc.*, 28, 559–573, 1987.
- Courtillot, V., C. Jaupart, I. Manighetti, P. Tapponnier, and J. Besse, On causal links between flood basalts and continental breakup, *Earth Planet. Sci. Lett.*, 166, 177–185, 1999.
- Cox, A., Confidence limits for the precision parameter K, *Geophys. J. R. Astron. Soc.*, 18, 545–549, 1969.
- Deniel, C., P. Vidal, C. Coulon, P. J. Vellutini, and P. Pigué, Temporal evolution of mantle sources during continental rifting: The volcanism of Djibouti (Afar), *J. Geophys. Res.*, 99, 2853–2869, 1994.
- Fischer, R. A., Dispersion on a sphere, *Proc. R. Soc. London, Ser. A*, 217, 295–305, 1953.
- Galibert, P. Y., B. Sichler, B. Smith, and N. Bonhommet, Paléomagnétisme en zone d'accrétion: Le cas de l'Afar, *Bull. Soc. Geol. Fr.*, 22, 881–890, 1980.
- Gillot, P.-Y., and Y. Cornette, The Cassinot technique for potassium–argon dating, precision and accuracy: Examples from the late Pleistocene to recent volcanics from southern Italy, *Chem. Geol., Isot. Geosci. Sect.*, 59, 205–222, 1986.
- Gruszow, S., Etude aéromagnétique et paléomagnétique du territoire de la République de Djibouti, Ph.D. thesis, 211 pp., Univ. Paris VII, Paris, 1992.
- Guyodo, Y., and J.-P. Valet, Relative variations in geomagnetic intensity from sedimentary records: The past 200 thousand years, *Earth Planet. Sci. Lett.*, 143, 23–36, 1996.
- Halls, H. C., A least-squares method to find a remanence direction from converging remagnetization circles, *Geophys. J. R. Astron. Soc.*, 45, 297–304, 1976.
- Halls, H. C., The use of converging remagnetization circles in paleomagnetism, *Phys. Earth Planet. Inter.*, 16, 1–11, 1978.
- Hofmann, C., V. Courtillot, G. Féraud, P. Rochette, G. Yirgu, E. Ketefo, and R. Pik, Timing of the Ethiopian flood basalt event and implications for plume birth and global change, *Nature*, 389, 838–841, 1997.
- Jacques, E., Fonctionnement sismique et couplage élastique des failles en Afar, Ph.D. thesis, 222 pp., Univ. de Paris VII, Paris, 1995.
- Johnson, C., and C. Constable, The time-averaged field as recorded by lava flows over the past 5 Myr, *Geophys. J. Int.*, 122, 489–519, 1995.
- Johnson, C. L., and C. G. Constable, The time-averaged geomagnetic field: Global and regional biases for 0–5 Ma, *Geophys. J. Int.*, 131, 643–666, 1997.
- Kidane, T., Contribution à l'étude paléomagnétique et géochronologique de l'évolution cinématique de la dépression Afar au cours des trois derniers millions d'années, Ph.D. thesis, 341 pp., Inst. de Phys. du Globe de Paris, Paris, 1999.
- Kidane, T., J. Carlut, V. Courtillot, Y. Gallet, X. Quidelleur, P. Y. Gillot, and T. Haile, Paleomagnetic and geochronologic identification of the Réunion subchron in Ethiopian Afar, *J. Geophys. Res.*, 104, 10,405–10,419, 1999.
- Kirschvink, J. L., The least squares line and plane and the analysis of paleomagnetic data, *Geophys. J. R. Astron. Soc.*, 62, 699–718, 1980.
- Lahitte, P., Le volcanisme Plio-Quaternaire lié aux mécanismes d'ouverture de la dépression Afar, Ph.D. thesis, 250 pp., Univ. Paris XI, Orsay, 2000.
- Lahitte, P., E. Coulié, T. Kidane, N. Mercier, and P.-Y. Gillot, K-Ar and TL volcanism chronology of the southern ends of the Red Sea spreading in Afar since 300 ka, *C. R. Acad. Sci.*, 332, 13–20, 2001.
- Lahitte, P., T. Kidane, V. Courtillot, A. Bekele, and P.-Y. Gillot, New age constraints on the timing of volcanism in central Afar, and implications on emplacement and rifting, *J. Geophys. Res.*, 108, doi:10.1029/2001JB001689, in press, 2003.
- Le Goff, M., Lissage et limites d'incertitude des courbes de migration polaire: pondération des données et extension bivariate de la statistique de Fisher, *C. R. Acad. Sci.*, 311, 1191–1198, 1990.
- Manighetti, I., Dynamique des systèmes extensifs en Afar, Ph.D. thesis, 242 pp., Univ. Paris VI, Paris, 1993.
- Manighetti, I., P. Tapponnier, V. Courtillot, S. Gruszow, and P. Y. Gillot, Propagation of rifting along the Arabia–Somalia plate boundary: The gulfs of Aden and Tadjoura, *J. Geophys. Res.*, 102, 2681–2710, 1997.
- Manighetti, I., P. Tapponnier, P. Y. Gillot, V. Courtillot, E. Jacques, J. C. Ruegg, and G. King, Propagation of rifting along the Arabia–Somalia plate boundary: Into Afar, *J. Geophys. Res.*, 103, 4947–4974, 1998.
- Manighetti, I., P. Tapponnier, V. Courtillot, Y. Gallet, E. Jacques, and P. Y. Gillot, Strain transfer between disconnected, propagating rifts in Afar, *J. Geophys. Res.*, 106, 13,613–13,665, 2001a.
- Manighetti, I., G. King, Y. Gaudemer, C. Sholz, and M. Doubre, Slip accumulation and lateral propagation of active normal faults in Afar, *J. Geophys. Res.*, 106, 13,667–13,696, 2001b.
- McElhinny, M. W., Statistical significance of the fold test in paleomagnetism, *Geophys. J. R. Astron. Soc.*, 8, 338–340, 1964.
- McFadden, P. L., A new fold test for paleomagnetic studies, *Geophys. J. Int.*, 103, 163–169, 1990.
- McFadden, P. L., and M. W. McElhinny, The combined analysis of remagnetization circles and direct observations in paleomagnetism, *Earth Planet. Sci. Lett.*, 87, 152–160, 1988.
- McFadden, P. L., and M. W. McElhinny, Classification of the reversal test in paleomagnetism, *Geophys. J. Int.*, 130, 725–729, 1990.
- McFadden, P. L., R. T. Merrill, M. W. McElhinny, and S. Lee, Reversals of the Earth's magnetic field and temporal variations of the dynamo families, *J. Geophys. Res.*, 96, 3923–3933, 1991.
- Prévot, M., and S. Grommé, Intensity of magnetization of subaerial and sub-marine basalts and its possible change with time, *Geophys. J. R. Astron. Soc.*, 40, 207–224, 1975.
- Odin, G. S., (Ed.), *Numerical Dating in Stratigraphy*, 2 vols., 1094 pp., John Wiley, New York, 1982.
- Quidelleur, X., and V. Courtillot, On low-degree spherical harmonic models of paleosecular variation, *Phys. Earth Planet. Inter.*, 95, 55–78, 1996.
- Quidelleur, X., J.-P. Valet, V. Courtillot, and G. Hulot, Long-term geometry of the geomagnetic field for the last five million years: An updated secular variation database, *Geophys. Res. Lett.*, 15, 1639–1642, 1994.
- Rochette, P., E. Tamrat, G. Féraud, R. Pik, V. Courtillot, E. Ketefo, C. Coulon, C. Hoffmann, D. Vandamme, and G. Yirgu, Magnetostratigraphy and timing of the Oligocene Ethiopian traps, *Earth Planet. Sci. Lett.*, 164, 497–510, 1998.
- Steiger, R. H., and E. Jäger, Subcommission on geochronology: Convention on the use of decay constants in geo- and cosmochronology, *Earth Planet. Sci. Lett.*, 36, 359–362, 1977.
- Tapponnier, P., R. Armijo, I. Manighetti, and V. Courtillot, Bookshelf faulting and horizontal block rotation between overlapping rifts in southern Afar, *Geophys. Res. Lett.*, 17, 1–4, 1990.
- Valet, J. P., T. Kidane, V. Soler, J. Brassard, V. Courtillot, and L. Meynadier, Remagnetization in lava flows recording pretransitional directions, *J. Geophys. Res.*, 103, 9755–9775, 1998.
- Varet, J., and F. Gasse, *Geology of Central and Southern Afar (Ethiopia and Djibouti Republic)*, Cent. Natl. de la Rech. Sci., Paris, 1978.
- Varet, J., et al., *Carte Géologique de l'Afar Central et Méridionale*, CNRS, Paris, 1975.
- Wilson, R. L., Dipole offset: The time-averaged paleomagnetic field over the past 25 million years, *Geophys. J. R. Astron. Soc.*, 22, 491, 1971.

L. Audin, V. Courtillot, Y. Gallet, T. Kidane, I. Manighetti, and X. Quidelleur, Laboratoires de Paléomagnétisme et de Tectonique, Institut de Physique du Globe de Paris, F-75230 Paris, France. (courtil@ipgp.jussieu.fr)

J. Carlut, Laboratoire de Géologie, Ecole Normale Supérieure, Paris, France.

P.-Y. Gillot and P. Lahitte, Laboratoire de Géochronologie Multi-Techniques UPS-IPGP, Bat.504 Sciences de la Terre, Université Paris XI-Paris Sud, F-91405, Orsay, France.

T. Haile, Department of Geology and Geophysics, University of Addis-Ababa, Addis-Ababa, Ethiopia.

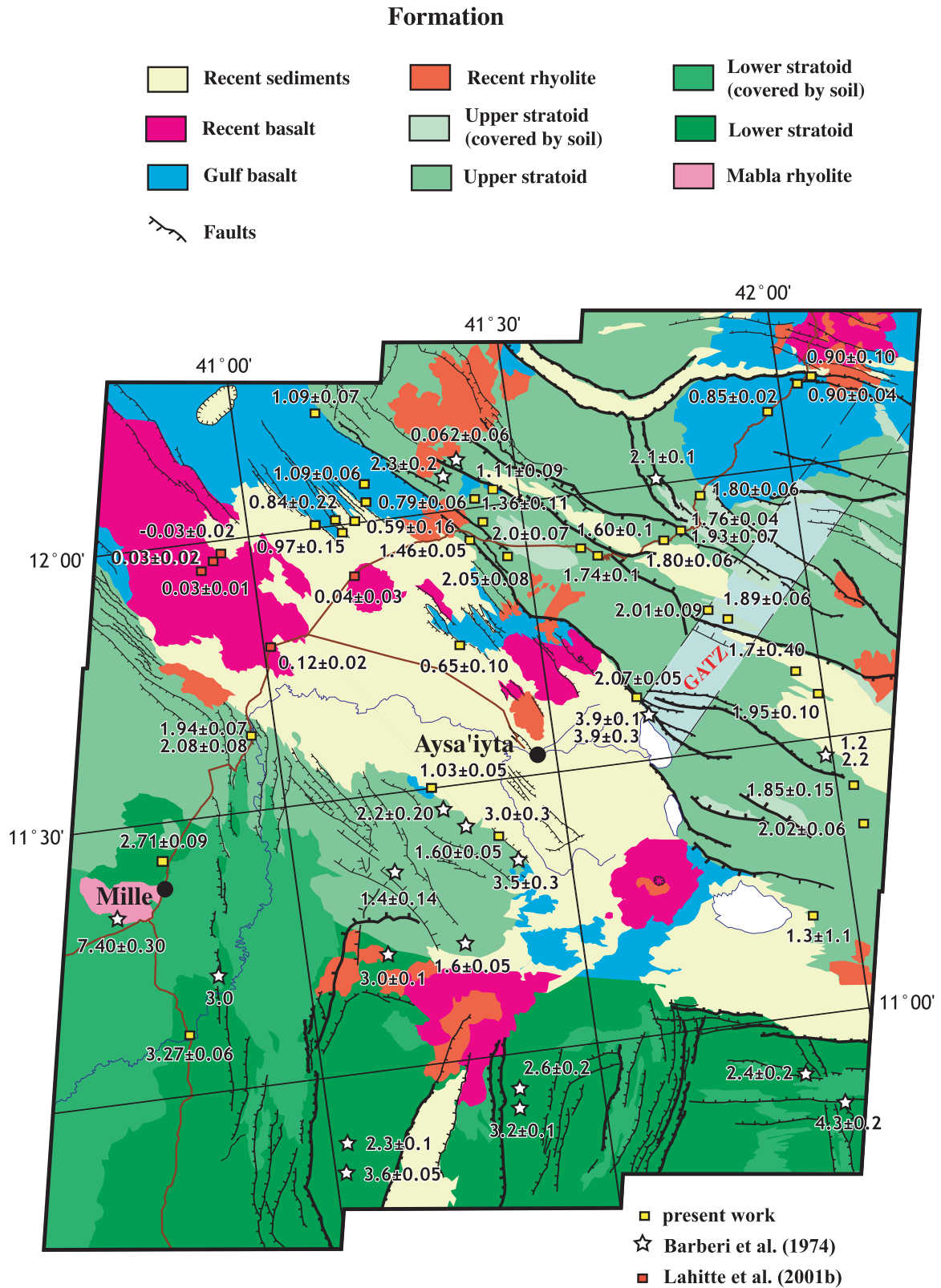


Figure 3b. Geological map of central Afar with main formations and faults and location of sites where an age determination has been obtained (yellow squares: K-Ar determinations (this study and earlier ones by our group); red squares: thermoluminescence data [Lahitte et al., 2003]; stars: K-Ar determinations [Barberi et al., 1975]; GATZ: Gamarril Alol tear zone).

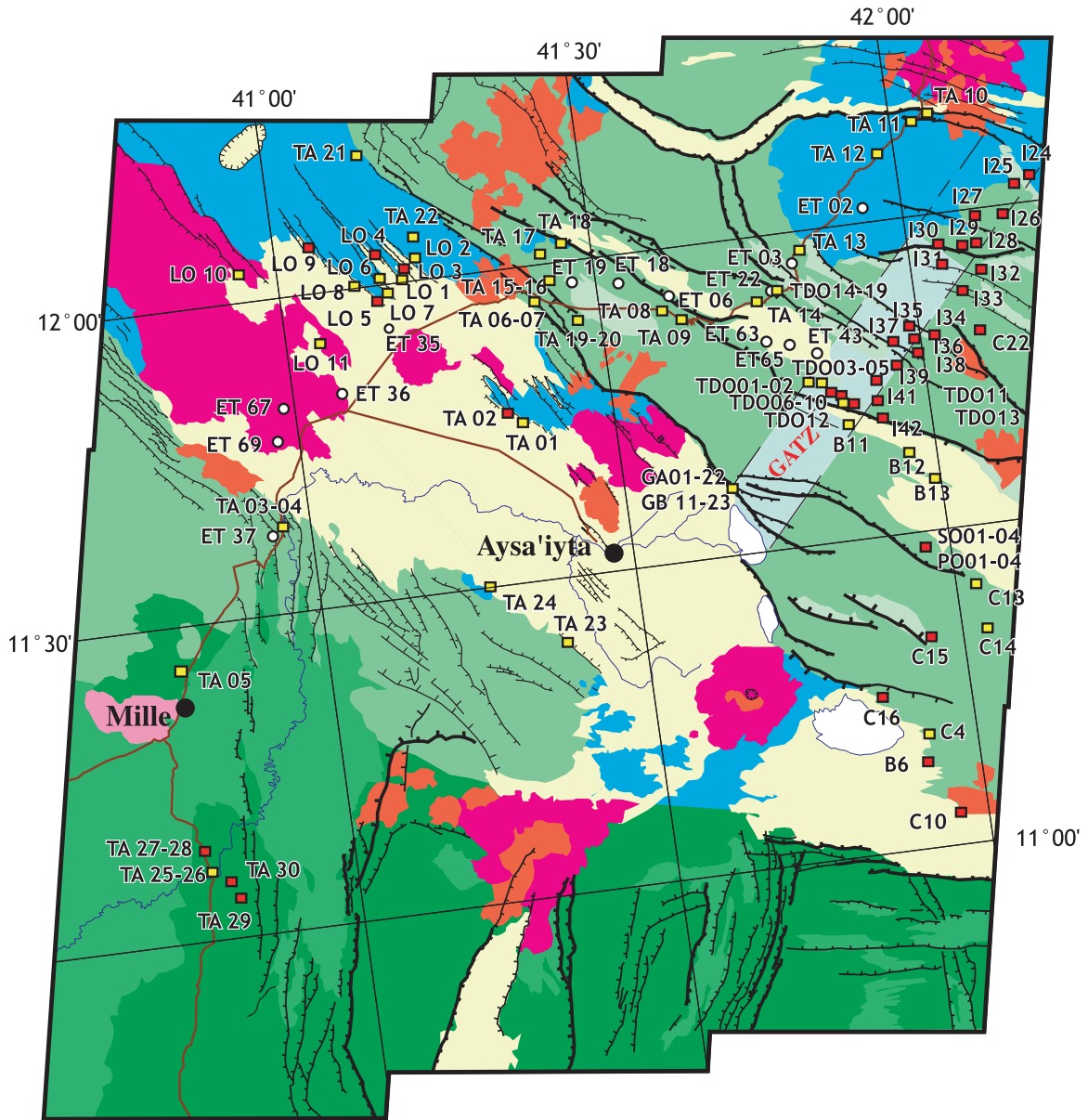


Figure 3c. Same as Figure 3b, with location of paleomagnetic sites: open circles are from the study of *Acton et al.* [2000]; squares are from our group [*Courtilot et al.*, 1984; *Manighetti*, 1993; *Manighetti et al.*, 2001a; this paper]: yellow squares are sites with a joint age determination and red squares are without one.